UNIVERSITÀ DEGLI STUDI DI PADOVA

DIPARTIMENTO DI INGEGNERIA INDUSTRIALE
CORSO DI LAUREA
MAGISTRALE IN INGEGNERIA CHIMICA E DEI PROCESSI INDUSTRIALI

Tesi di Laurea Magistrale in Ingegneria Chimica e dei Processi Industriali

COLD PLASMA TREATMENT OF NYLON 6,6 TEXTILE TO IMPROVE FLAME RETARDANCY

Relatore: Prof. Ing. Alessandra Lorenzetti
Correlatore: Prof. Baljinder Kandola

Laureanda: Arianna Vendrame

ANNO ACCADEMICO 2017-2018

Abstract

The main objective of this work is to enhance the flame retardancy of Nylon 66 textile by improving the effectiveness of the flame retardants treatment, i.e. the amount of flame retardant uptake. One possible solution might be the usage of plasma to activate the fabric surface in order to increase the add-on amount of flame retardants. Two types of cold plasma equipment have been investigated: microwave atmospheric plasma using Ar and Ar/O_2 gases and vacuum plasma using He/O_2 gas. First preliminary results have shown that better functionalisation can be obtained by vacuum plasma machine, and therefore the study has proceeded analysing deeply this kind of treatment .

The effect of several process parameters (power, time, ionized gas composition) on the effectiveness of the subsequent flame retardant treatment (pad-mangle method) involving the dipping into thiourea solution, has been analysed. The results showed that the add-on content of thiourea can be improved by the vacuum plasma functionalisation of the textile, thanks to the increase of the concentration of polar groups on the surface, as shown by FTIR analysis. Because of the higher add-on content, it has also been shown that the limiting oxygen index of functionalised fabrics was higher than that of unfunctionalised ones, thus proving the effectiveness of plasma treatment in enhancing fire behaviour of Nylon textile. At the end, by using a DOE methodology, after finding a suitable quadratic model, an optimized set of process parameters has been identified and validated by experimental trial.

Riassunto

L'obiettivo principale di questo lavoro è di aumentare le prestazioni al fuoco del tessuto Nylon 66 migliorando l'efficacia del trattamento con i ritardanti di fiamma, come per esempio l'assorbimento di ritardante. Una possibile soluzione può essere l'utilizzo del plasma per attivare la superficie del tessuto in modo da aumentare l'assorbimento dei ritardanti di fiamma. Due tipi di strumenti per il plasma a freddo sono stati presi in esame: il plasma atmosferico a microonde usando come gas Ar e la miscela Ar/O_2 e il plasma sottovuoto usando come gas la miscela He/O_2. Risultati preliminari hanno prima dimostrato che può essere ottenuta una miglior funzionalizzazione con lo strumento sottovuoto, e quindi lo studio è proceduto analizzando in maniera approfondita questo tipo di trattamento.

È stato studiato l'effetto di diverse variabili di processo (potenza, tempo, composizione del gas ionizzato) sulla efficacia trattamento con il ritardante di fiamma (metodo *pad-mangle),* che prevede l'immersione del tessuto nella soluzione di tiourea. I risultati hanno mostrato che il contenuto di tiourea può essere migliorato con la funzionalizzazione del tessuto con il plasma sottovuoto, grazie all'aumento della concentrazione di gruppi polari sulla superficie, come dimostrato dall'analisi FTIR. Grazie all'aumento dell'assorbimento, è stato dimostrato anche che l'indice di ossigeno dei tessuti funzionalizzati era più alto di quelli non funzionalizzati, quindi provando l'efficacia del trattamento al plasma nel miglioramento del comportamento al fuoco del tessuto di nylon. Alla fine, usando la metodologia DOE, dopo aver trovato un modello quadratico appropriato, un set ottimizzato di parametri di processo è stato identificato con una verifica sperimentale.

Index

Introduction

The particular hazard posed by burning textiles (like as clothing or textile for domestic environment) is known since long. In many large-scale fires, the textiles present at each scene have been the material ignited first by the relevant igniting source. It shall also be considered that the fire behaviour of textile used in public environment (e.g. hotel, airport, public building) is very important to guarantee the safety of the people staying inside. Finishing technologies are a way to confer flame retardancy to textile when the fiber/fabric is impregnated by a solution containing a flame retardant. However, flame retardants are costly and, in some cases, toxic and therefore there is a need to reduce their use but still maintaining the same level of flame retardancy. Plasma processing can be used to modify surface of textile by etching, functionalization, plasma coating (grafting) and desizing. The modified surfaces can be made either hydrophilic or hydrophobic depending on the selection of appropriate gas or precursors to form plasma as well as plasma reactor conditions. Surface modification, as a sole process or as a pre-treatment, can effectively be used for functional finishing of textile materials; for example, special finishes such as antistatic and antisoiling finish for synthetics, flame retardant and water-repellent finishes for cotton can be imparted using this treatment.

Therefore, in this work we'll analyse the use of plasma processing to modify nylon textile surface and improve the flame retardant uptake (in particular thiourea) during the finishing process. The main aim is to be able to reduce the concentration of thiourea needed to reach a certain degree of flame retardancy. Since the limiting oxygen index (LOI), has proved to be a very effective indicator of ease of ignition, it will be used to assess the usefulness of plasma treatment in promoting flame retardancy of Nylon 6,6 textile.

Now we present the structure of the thesis, in order to point out the main points. In the first chapter we give some information regarding thermoplastic and thermosetting polymers, in particularly about the polyamides. Then we proceed with the description of Nylon 6,6 synthesis and its degradation process; fibres are formed through the melt spinning process. A general view of their field of application is given in the following §. In chapter 2 we explain how plasma works, focusing on the two microwave equipment used for this study. Later we illustrate the modifications caused on surface polymers thanks to this type of treatment. In chapter 3 instead we present the main characteristics of flame retardants, the different modes of action and their classification, with then more attention for thiourea compound, the favorite flame retardant for Nylon 66. In chapter 4 we give an overview of the instruments used in the experimental part; we use the FTIR and TGA instruments; then we explain how we obtain the LOI value to evaluate the fire performances of the textile, that will be treated in different ways. We also show the UV-Vis spectroscopy equipment to understand the DPPH analysis presented in the following chapter. SEM operating principles are given, indeed morphological information is needed to study Nylon surface; the last method is the capillarity test, to see if plasma can increase liquid rise on the material. In chapter 5 and 6 we explain the experimental part of this thesis. In chapter 5 we describe in detail the atmospheric and vacuum plasma instruments and the related analyses performed on the fabric. For the atmospheric machine we analyse Nylon exploiting DPPH analysis, SEM images, FTIR spectra. Concerning the vacuum plasma equipment, we evaluate the best conditions to treat our woven thanks to capillarity test and FTIR spectra; in this way we choose the values for time, power and the gas ratio of He/O_2 mixture. TGA plots of nylon and of the processed one are reported as well. In chapter 6 we present the results concerning the DOE study, to find the values for time and power that can guarantee the highest improvement of LOI with respect unfunctionalized nylon, using the vacuum plasma equipment. Considerations will be done to assess if plasma is effectively working in improving LOI values, and if it happens, we should justify this behaviour.

Chapter 1

Polymeric materials and Nylon 66 fibres

In this chapter we deal with a generic explanation about polymeric materials and, particularly, about polyamides, since the topic of this dissertation concerns PA 66. Then we proceed focusing only on Nylon 66 fibres. First we illustrate the principal characteristics and the degradation process of this material, then the process to obtain these fibres. At the end we introduce the field of application of this thermoplastic polymer.

1.1 Polymeric materials

Polymeric materials, in other words plastics, are formed by monomeric units bounded together to form a linear chain or macromolecule. Usually polymers are constituted by organic macromolecules. They are divided into natural (cotton, cellulose, proteins) and synthetic polymers (nylon, PE, polyesters, polyisoprene). Their properties can be defined from the number of the structural units that form the macromolecule and from the weak interactions between macromolecules.

The degree of polymerisation, that is the total number of monomeric units of one macromolecule, and the molecular weight are two important parameters related to polymers.

They can be distinguished in two big groups: thermoplastic and thermosetting polymers.

Thermoplastic polymers can be easily re-formed, by increasing temperature we obtain a viscous liquid, and by cooling they are solid again. So, their formation process is reversible. For example, nylon is a thermoplastic polymer.

Instead *thermosetting polymers* are formed in presence of a cross-linking agent, and irreversible chemical bonds are formed; this is called curing process (hardening of a polymer). They are insoluble, infusible cross-linked polymers, that do not soften after further heating, actually they

decompose; this means that the transition from solid to liquid state is irreversible. For rubber, the curing process is called vulcanisation.
Increasing the number of reticulations, the rigidity increases, they are stronger than the previous ones; because of the three-dimensional crosslinking and covalent bonds they cannot easily break. They are characterised by a fragile behaviour as opposed to thermoplastic polymers. They are used for their thermal and dimensional stability when heated.

To conclude, thanks to their easy processability, low cost, and the many fields of application, polymers are so important nowadays in our life.

1.2 Polyamides and their main characteristics

Polyamides are thermoplastic polymers that belong to the *Engineering Plastics (tecnopolymers)*, therefore they are characterised by high performances; these polymers can support high temperatures, bending, vibration, friction tests, and so on.
These polymers are produced either by reaction of a diacid with a diamine or by ring-opening polymerisation of lactams. They contain the characteristic amide group CO-NH. Both N-H and C=O are polar groups, hence secondary bonds between adjacent macromolecules are formed (Fig. 1.1). Thanks to these hydrogen bonds, these polymers have high tensile strength, very good hardness, high wear resistance; since the molecules absorb water, they are able to deform and to resist the impact, in fact water acts as plasticiser.
Moreover, their structure determines the high degree of crystallisation, and this is responsible for the good mechanical properties of polyamides. These features are useful in the field of fibres, automotive parts, industrial valves and other industry uses.

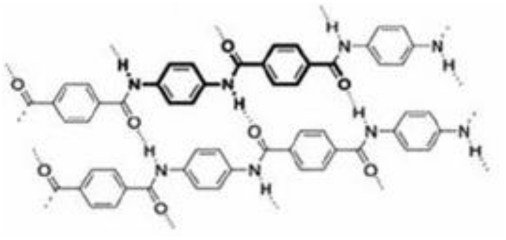

Fig. 1.1: *Hydrogen bonds and characteristic group in polyamides*

In the following paragraph we discuss about the different structures that polyamide can have.

1.2.1 Classification of polyamides

Polyamide polymers can be subdivided into three groups: aliphatic, semi-aromatic, fully aromatic thermoplastics.

- Aliphatic polyamides or *Nylon*: the most important are Nylon 66 and Nylon 6. They have good mechanical performances, given that they have high melting temperature and glass transition temperature. The main limitations are the moisture sensitivity and the resulting change in mechanical properties.
- Aromatic polyamides or *aramids*: they include an aromatic functional group in the monomer structure. This class of polymers has unique properties, indeed the aromatic content reinforces the material; they do not burn, they are resistant to solvents at room and elevated temperatures and they melt at high temperatures, thanks to the strong bonds between aramid chains. The most known aramid is Kevlar®, which is used to do bulletproof vest. Compared to Nylon, Kevlar and Nomex fibres are much more crystallised and rigid. Moreover, aramidic fibres can undergo deformation before breaking, indeed they are more tough than carbon or glass fibres.

1.3 Structure and properties of Nylon 66

Nylon 66 has excellent compressive resistance and tensile strength (85 MPa), especially when the polymer is drawn into fibres. In Fig. 1.2 we can see the crystalline form, generally this structure is in combination with the amorphous phase, so that PA66 is a semi-crystalline polymer.

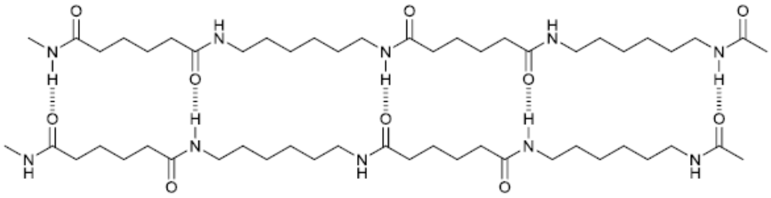

Fig. 1.2: *H-bonding in Nylon 66*

1.3.1 Synthesis of PA66

W. H. Carothers in 1930's invented the synthesis of Nylon 66, the first synthetic polyamide.

At first, Nylon is the chosen name for polyamide fibres for DuPont, but since it is not a registered trademark, it has become the general name also for polyamides with other structures. This polymer is synthesised from hexamethylenediamine and adipic acid, these two components in equal proportion are melted in water to produce an ionic solution, called 'Nylon 66 salt'. After treatment of activated carbon to remove impurities, the mixture is heated to reach higher temperatures, and the excess water is removed by evaporation, as we can see from Fig. 1.3 [1]. This salt is transferred to a continuous polymerisation reactor, PA66 is produced with a polycondensation reaction carried on at 280°C under pressure (at ambient pressure the melting point is 264°C). Then the pressure goes down to 1 atm and water is removed to reach the desired molar mass.

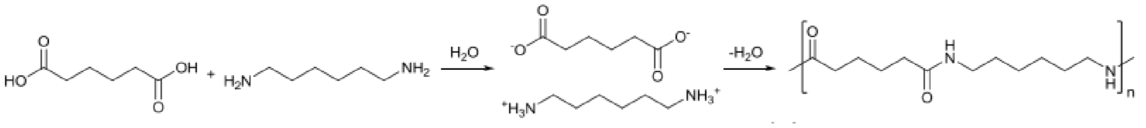

Fig. 1.3: *Schematic synthesis of Nylon 66* [1]

Usually the degree of polymerisation is about of 80-150 units; in non-textile fields higher molecular weight may be necessary, that is instead a problem in textile sector.

1.4 Degradation mechanism of Nylon 66

To understand the relative thermal stability of polymers we refer to the temperature at which they lose half of their starting mass, that is T_h [2].

This polyamide can be heated to about 280-290°C, because at 305°C it leads to formation of 3-dimensional structures and gel formation. Indeed, a problem occurring for Nylon 66 is that during melt extrusion interruptions are needed after few hours to avoid obstructions. Instead for Nylon 6 the extrusion can proceed for days before it gels. These gelling effects are due probably to formation of cyclopentanone sub products and reactions involving these derivatives.

Now we present the nonoxidative thermal degradation, that occurs in an oxygen-free environment, and the photo-oxidative degradation, in presence of oxygen and light.

1.4.1 Nonoxidative thermal degradation

Random chain scission is the principal decomposition process of polyamides, illustrated in Fig. 1.4 [1].

Fig. 1.4: *General reaction for random chain scission* for an aliphatic polymer

A lot of products, like the monomer, are the result of this process; breaks at random points leads to different species.

End chain scission, called also depolymerisation, is in addition to the random chain scission (illustrated in Fig. 1.5). In this case there is a break at the end of the chain, leading to the loss of monomer units.

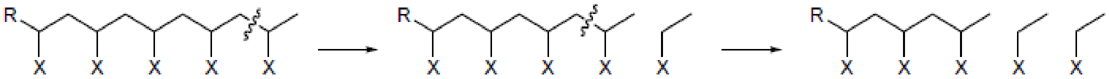

Fig. 1.5: *General reaction for end chain scission* for an aliphatic polymer

Breakings occur at -NH-CH_2- bond, to give ammonia, carbon dioxide, carbon monoxide, cyclopentanone and its derivatives, cyclohexane, indeed during degradation ring-forming is very common to be observed.

Also isocyanate groups have been reported in thermal degradation of Nylon 66, and not for Nylon 6, as we can see from Fig. 1.6 [3]:

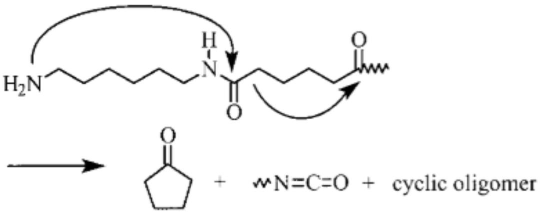

Fig. 1.6: *Mechanism of thermal degradation for Nylon 66 with intra-molecular end-biting*

Now we want to address this topic more specifically showing the reactions leading to these compounds, by referring to **model compounds** studied in the last 60 years.

- Formation of cyclopentanone and isocyanate is shown in Fig. 1.7 [1]:

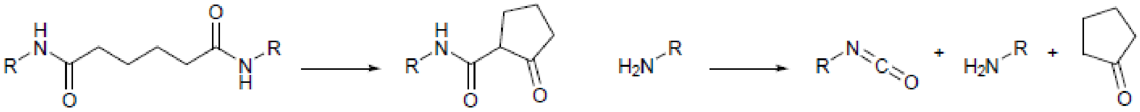

Fig. 1.7: *Intramolecular reaction in PA66*

- In Fig. 1.8, instead, we report the one that is commonly accepted as the primary chain scission, that leads to production of free amide and C=C bond.

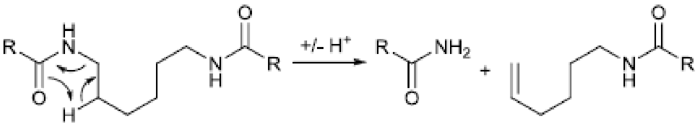

Fig. 1.8: *Degradation of model PA66 hexamethylene diamide*

- Cross-linking causes condensation mechanisms, leading to ammonia; secondary amines derive from primary amines, and then we obtain tertiary amines from cross-linking of secondary and primary amines. So, we can allocate the formation of ammonia to cross-linking that occurs in Nylon 66, as we can see from Fig. 1.9.

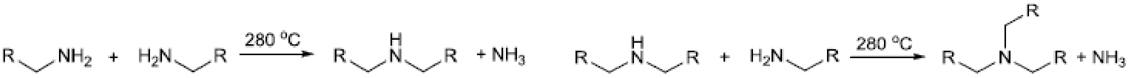

Fig. 1.9: *Cross-linking in PA66*

1.4.2 Photo-oxidative degradation

In presence of oxygen the decomposition process proceeds faster, because it can react with carbon present along the chain; first we observe the formation of polymer alkyl radicals thanks to thermic energy, then the degradation goes further and leads to the formation of peroxide radicals caused by the presence of oxygen. In turn, ROOH catalyses other degradation reactions at T higher than 120°C. We can see the general mechanism that involves also polyamides in Fig. 1.10.

Initiation: $RH \xrightarrow{\Delta} R^{\bullet} + {}^{\bullet}H$

Propagation: $R^{\bullet} + O_2 \rightarrow RO_2^{\bullet}$

$RO_2^{\bullet} + RH \rightarrow ROOH + R^{\bullet}$

Termination: $R^{\bullet} + R^{\bullet} \rightarrow R\text{-}R$

$RO_2^{\bullet} + R^{\bullet} \rightarrow ROOR$

$RO_2^{\bullet} + RO_2^{\bullet} \rightarrow \text{Products}$

Chain branching: $ROOH \rightarrow RO^{\bullet} + {}^{\bullet}OH$

Fig. 1.10: *The general Bolland and Gee reaction scheme for a polymer oxidation*

When photo-oxidation occurs, the radical reactions are analogous to those reported in Fig. 1.10. As the mechanism suggestes for photo-oxidation of polyamides [4], the decomposition of hydroperoxides leads to the production of carbonyl groups, as we can see in Fig. 1.11:

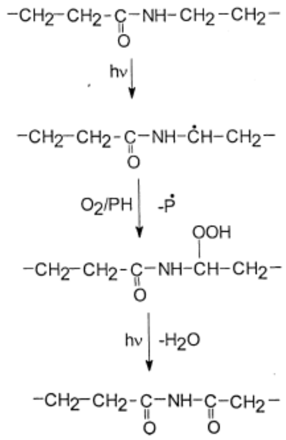

Fig. 1.11: *Photo-oxidative degradation mechanism for polyamides proposed by Do et al.* [4]

According to those studies, there is a single photo-oxidation mechanism during the process, that leads to an increase in carbonyl group concentration. For polyamides the primary photo-oxidation involves the oxidation of methylene group adjacent to -NH- group. Moreover, the diffusion of oxygen is related to the structure of the polymer: its presence involves mainly the amorphous phase, it decomposes continuously with exposure time. Oxygen has difficulties in diffusing in the crystalline phase, indeed the structure is more rigid and more packed.

In the following paragraph we explain the process to obtain Nylon 66 fibres, starting from Nylon chips.

1.5 Nylon fibres and melt spinning

In the textile industry Nylon 66 is most diffused in Nord America, compared to Nylon 6 fibres that are instead more common in Europe.

For the fabrication of Nylon fibres (see Fig. 1.12), we start from chips, or pellets (3-5 mm) that are melted at a temperature of around 300°C; then the polymer is extruded through a *spinneret*, a die composed of multiple orifices; the molten polymer is pumped at a constant pressure to form fine filaments. The application of optimum shear rates and frequent mixing of the melt are necessary. The molten material must be continuously cleaned and purified to avoid obstructions (they cause weak points), so it goes through a filter called screen pack. The fibres are drawn to their final diameter, stretched to the required diameter and solidified in a water bath or by forced convection. The drawing procedure is required to enhance fibre properties, like tensile strength and stiffness. This process is called *melt spinning*, in particular *normal spinning*. This is possible because Nylon can melt without degrading. As follows we list the principal moments of this process [5]:

- Feed: after the melting of chips in the extruder, the material passes through the spinneret at a controlled pressure and temperature. There are some pumps that control the polymer flux. Before the stretching, the polymer reaches a T higher than the glass transition T, so that there is mobility of the macromolecules.
- Spinneret: these dies are realised in metal alloy, which can resist high P and corrosive materials.
- Collection: after the cooling, the yarn is collected in control rolls and drive rolls, and then the drawn yarn is wounded up in the bobbin and strained to have partial orientation.

The product of spinning process is called P.O.Y., or Pre-Oriented Yarn, which can have different shapes of section. This is further subjected to other processing techniques, from an aesthetic, functional and tactile point of view. Then it is necessary to stretch and extend the yarn, so the molecular chains are parallel.

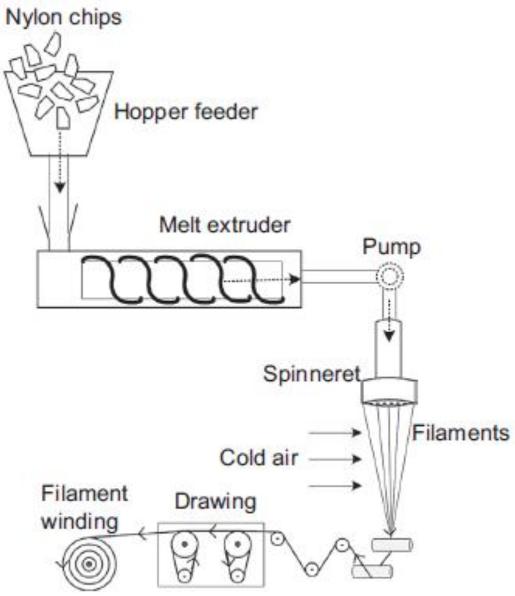

Fig. 1.12: *Production of nylon filament yarn by melt spinning*

1.6 Fields of application of Nylon 6,6 fibres

Nylon 66 was firstly used to produce a pair of socks, presented from DuPont in 1939; since they were tough and brilliant, this company had a huge success. This fibre was commercialised with the slogan 'tough as steel, thin as spider web, but more elastic than all common natural fibres'. Besides, these fibres were used during Second World War in USA for war purposes, to realise parachutes. Later, it was employed again for aesthetic purposes. In the 50's Nylon was more utilised than silk. DuPont offers a wide range of PA66 for use in industrial, textile, furnishing covering applications.

- Since Nylon has good abrasion resistance it is used for carpets, conveyor belts;
- Thanks to its high melting point it plays a part in rubbery industry for high-T tyre curing;
- It plays a part as warp knitting in apparel sector;
- It is employed in packaging for film sheet;

In particular we want to focus on textile industry. Nylon fabrics are used for hosiery products when they are made of 15 denier monofilaments, indeed they are characterised by good elastic recovery. In general, Nylon filament is widely used in dress sector, for example wool is blended to improve its durability, especially in the case of overclothes or floor coverings. In addition, this technical textile is used for tyre cords for trucks, airplanes, then also for sail clothes, canvas for luggage.

For this project it is important to highlight another application of this polymer. From 1940s military world has employed Nylon 66 in different components of soldier equipment: military wear can be light and can have high tearing strength, then backpack, stay cord, military footwear.

Chapter 2

Cold plasma treatment

In this chapter we want to explain in detail what cold plasma is, why it is used, and to highlight its applications in textile sector. First of all, it is a dry, environmental, worker-friendly method that can be divided into atmospheric and vacuum plasma; both of them have advantages and disadvantages that we are going to list. We are interested in the equipment employed in textile sector, since we deal with Nylon 66 fabric.

2.1 Main characteristics of cold plasma

Plasma is an ionised gas, electrically neutral because the positive and negative charges offset each other; it is an electrically conducting medium.

Increasing the temperature, we pass from solid state, to liquid state, then to gaseous phase, and finally to plasma condition; it is composed by excited atomic, molecular, ionic and radical species with free electrons and photons. It is required to provide enough additional energy to gases; if energy is sufficient, a bond electron may be excited, and it becomes a free electron, hence the atom is ionised. The minimum required energy to free an electron is called ionisation energy. As we can notice in Fig. 2.1, charged particles are emitted when electrons bump into neutral particles of the gas. One possibility to generate plasma is thermal energy, another one is the application of an electric field to a neutral gas.

In cold plasma temperature of electrons can reach also 30000 K, but the bulk temperature is approximately equal to the ambient one.

The interactions between particles are at long radius; every charged particle is influenced by all other ones, so it means that plasma behaves like a unitary fluid.

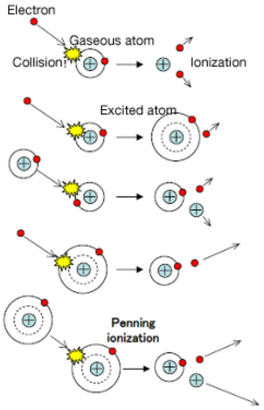

Fig. 2.1: *Electron impact ionisation*

Electron density indicates how many electrons are in a given volume, so it is not related to the electrons bounded to an atom, but to the free electrons. It depends on three parameters: the electrical conductivity, the electron charge and electron mobility, that is proportional to the velocity of charged species in an electric field.

In plasma gas, elastic and inelastic collisions are involved, atom-atom, electron-atom, ion-atom collisions are elastic when total kinetic energy is conserved, instead in the inelastic ones potential and kinetic energy are exchanged. In plasma process Coulomb collisions between charged particles are the prevalent ones, they are elastic impacts and long-range forces.

2.2 Different plasma production using electric fields

The goal of this paragraph is an explanation of different types of plasma generation; these following plasma sources are all generated using an external electric field that causes the decomposition of the gas. Since this work deals with microwave source (either atmospheric or vacuum), we will focus on this one.

- *Dc glow discharge plasma*: it is generated using interior electrodes, which can be of different types depending on the applied voltage and discharge current. Free electrons are accelerated from the cathode towards the anode, so they acquire energy to detach electrons from neutral molecules. To allow collisions between electrons and neutral species the voltage between cathode and anode must be sufficiently high. For plasma applications dc discharges can be continuous, or pulsed, which has some advantages, like the possibility to operate at higher power.

- *Radio frequency plasma*: it is necessary to apply a radio frequency field to a gas. The selected frequency range is 1-100 MHz, with wavelengths of 300-3 m. It can operate over a high interval of pressures.
- *Microwave plasma*: the excitation is different from the previous case, sources' frequency value is higher than 300 MHz, normally the selected one is 2450 MHz. Microwave discharge can work either under vacuum or at atmospheric pressure.
- *Dielectric barrier discharge*: it operates at atmospheric pressure; for example there is a plasma equipment in Huddersfield, UK, that aims to treat and functionalise textiles at atmospheric pressure and at an industrial scale. The advantage is that the vacuum equipment is not needed, reducing the operating costs.

We can distinguish between the power absorption and the power reflection, and of course the objective is to minimize the second one, indeed it indicates the lost power during the generation plasma process. The power absorption can be calculated using Eq. 2.1 [6]:

$$\frac{P_{abs}}{V} = \frac{1}{2} n_e \frac{e^2}{m_e \nu} \frac{\nu^2}{\nu^2 + \omega^2} E_0^2 \qquad (Eq. 2.1)$$

where n_e is electron density, e and m_e are respectively electron charge and mass, ν electron collision frequency, ω the angular frequency of electromagnetic.

2.2.1 Microwave plasma

The principal components of microwave plasma are power supply, a circulator, the applicator and the plasma load; the applicator has the goal to minimise power reflection and therefore to maximise the transferred energy into plasma gas.

Plasma density depends on microwave power and pressure, microwave plasmas are characterised by high density, especially at a pressure of 0.1 mbar; they work up to the atmospheric pressure; moreover a higher number of electrons that can cause ionisation is generated with this source.

First, we list the process parameters of the *microwave atmospheric plasma* used for this experimental part; the structure is simple and costs are lower because no equipment for vacuum generation is needed.

- Number of scans: number of forward and backward paths of the flame over the material. The flame passes on the surface with a certain distance and the switch from forward to backward path is automatic;
- Distance of the material from the nozzle: it depends on the treated material, decreasing the distance the treatment is more efficient, but we must be careful not to damage or burn the sample;
- Type of gas used for the ionisation and its flow-rate [cm^3/min]: flowmeter is present for the regulation;
- Forward power [W]: increasing the power also the electron density grows. The maximum forward power that we can apply in the equipment used for this study is 300 W. In Fig. 2.2 we can notice how the regulation occurs;

Fig. 2.2: *Microwave power supply to regulate the power*

Concerning the *vacuum microwave plasma,* the processing parameters are the following:

- Pressure [mbar]: we regulate the flow of gas entering the reactor to control the pressure. At low pressure collisions between particles are fewer than using high pressure, so the gas is less reactive. In this case the costs are more relevant;
- Power [W]: the density of the plasma increases with power;
- Distance of the sample from the lamp;
- Time of treatment [s]: it depends on the material inside the chamber, on the power and on the gas used. For example, it is possible to establish the necessary time to increase

wettability on textiles measuring the contact angle, the time that guarantees the maximum contact angle is the one needed for that fabric;

- Type of gas and flow-rate [cc/min]. As explained later, depending on the project target a proper gas has to been selected;
- Frequency [MHz]: usually it is selected between the range 2450-2470 MHz.

In Fig. 2.3 we report two pictures related to this type of reactor and Fig 2.4 displays where we can change the parameters mentioned above:

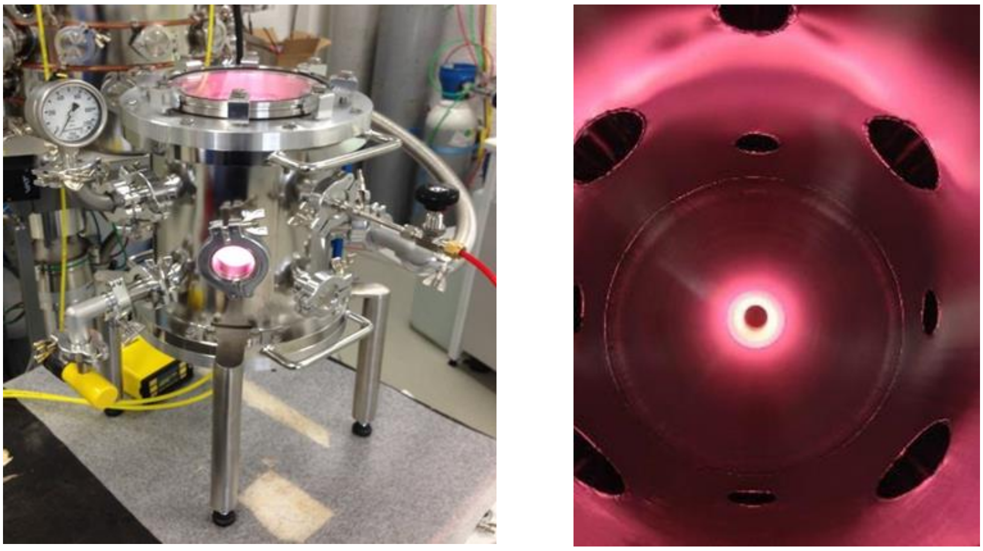

Fig. 2.3: *Microwave vacuum plasma equipment and light generated by plasma inside the reactor*

Fig. 2.4: *Pro-face for touch display*

2.3 Four modifications performed for fibres and polymer surfaces

In textile industry plasma device is useful to modify the polymeric fibres and their properties avoiding high water usage and limiting their damage.

We can distinguish between three main categories for plasma gases: inert gas plasmas, oxygen plasmas and nitrogen-containing plasmas.

In general, the principal aim is to change the surface to a high-energy state and to generate polar groups.

Below we report some general information about the main effects of plasma on textile surfaces:

- *Cleaning and etching* (ablation): thanks to the ablation of the treated material volatile products are formed, oxygen containing plasma removes organic contaminants from polymer surfaces, producing volatile species. Indeed, contaminants like oils withstand hydrogen abstraction caused by radicals, ions, electrons present in the plasma.

  As regards the etching process, along polyamide structure C-H, C-N, C-C, N-H groups are subjected to chain breaking. In presence of air or oxygen methylene carbons adjacent to the amide carbonyls are oxidised.
- *Activation* surface changes to a high-energy state because of the increase in surface tension and formation of polar groups. Free radicals created on polymer surface are caused by chain scission, represented in Fig. 2.5 [7]:

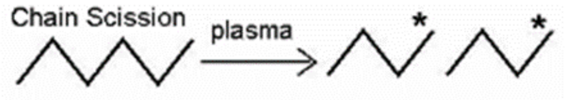

Fig. 2.5: *Radicals produced during treatment*

Inert gases as He and Ar are not reactive gases, but they can abstract hydrogen and form free radicals, interacting to form crosslinks. Different new functional groups can be introduced into the surfaces depending on the gas used, a large variety of final purposes can be achieved; for example, ammonia gas plasma is able to provide nitrogen functionalities as $-NH_2$, -CH=NH-, compared to oxygen gas plasma that produce C-O-O, C=O, O-C=O. Fig. 2.6 shows the general process for the formation of these groups [7]:

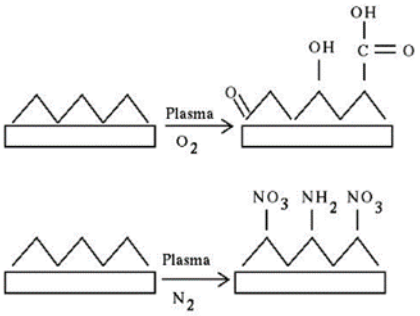

Fig. 2.6: *Surface activation of a general polymeric surface*

For instance, the goal of the activation of technical polymers is the adhesion of coatings.

- *Grafting*: one possible advantage of using plasma technique is to bond a monomer on the textile structure with covalent bonds; in this case the monomer (usually acrylic acid, amine) is introduced inside the chamber where the plasma is generated. The monomer can react with the radicals produced on the material and is grafted to the surface. In this way it is possible to change the properties of the polymer, and for example its wettability is enhanced. Usually bond permanency is achieved, and the adhesion is not damaged by external factors.
- *Dyeing and printing*: thanks to oxygen plasma treatment the capillarity of some materials increases [8]. Below we show Eq. 2.2-2.7 ion and electron generation, radicals' formation, and final products of heat and light occurring with oxygen plasma. This plasma can increase wettability of textile, dyeing, thanks to the excited state of O_2 and O (O_2^*, O^*).

$$e^- + O_2 \rightarrow O_2^+ + 2e^- \qquad (Eq. 2.2)$$

$$e^- + O_2 \rightarrow O + O \qquad (Eq. 2.3)$$

$$e^- + O_2 \rightarrow O_2^* + 2e^- \qquad (Eq. 2.4)$$

$$O_2^* \rightarrow h\vartheta \qquad (Eq. 2.5)$$

$$e^- + O \rightarrow O^* \qquad (Eq. 2.6)$$

$$O^* \rightarrow h\vartheta \qquad (Eq. 2.7)$$

Chapter 3

Flame retardants

In this chapter we will face a general view of the combustion cycle of polymers, and the principal steps of Nylon 66 burning mechanism; then we will focus on the main features of flame retardants and their mechanisms of action, their use for textiles, and especially polyamides. Finally, a separate explanation about thiourea is necessary, since this work deals with this compound.

3.1 Combustion of polymers and generic flame retardants

Combustion is a chemical reaction of oxidation, generating light and heat.

As follow we want to explain the combustion cycle of polymers, indicated in Fig. 3.1. When the polymer is degrading products are in gas phase, heat is released and in this way the combustion is self-sustaining. To have combustion the gas mixture must stay within flammability limits. The combustion is based on **4 stages**: pre-heating, ignition, combustion and propagation. So, when these passages occur, the released heat is very high and it is partially transferred to the polymer; if decomposition velocity is sufficiently high and the concentration of volatile components stays within combustion range the cycle is self-sustaining and so the polymer still burns.

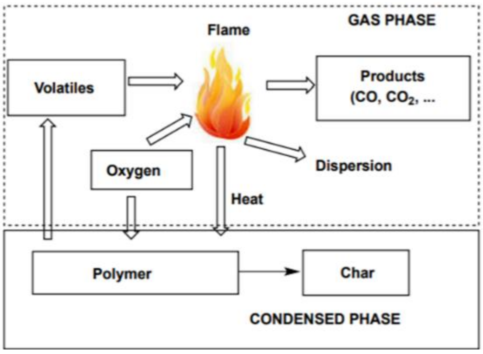

Fig. 3.1: *Combustion cycle for a polymer*

Here below we indicate the burning mechanism of polymers, in particularly of Nylon [9]:

- Initiation: in this first stage an external source (like a flame) is involved, this supply of energy brings a temperature increase and leads to the following steps;
- Primary and Secondary Decomposition: weak bonds start to break, early pyrolysis occurs up to 350°C involving random bond scission. After rupture of Nylon chains oligomers are formed, C-N bond is involved in the primary decomposition. Then, the secondary decomposition comes after; depolymerisation to monomer takes place (as explained in chapter 1). Volatile fuels are generated, having C-C bond rupture too. (450-470°C). Literature reports that both homolytic and hydrolytic cleave are present.
- Ignition: the ignition of Nylon is at 421-425°C (when a source is present); instead the autoignition point is when Nylon spontaneously ignites.
- Combustion and propagation: we have a gas-phase reaction that involve other regions of the material; it can proceed thanks to an external source and then it stops, or it can auto-propagate. In the case of Nylon, a free-radical oxidation influences the all process, with temperature higher than 500°C a rapid decomposition of this polymer to volatile species happens. The combustion is affected by different parameters: geometry of the surface, decomposition velocity and transfer velocity of heat and combustion heat of the polymer, in general the generated heat that can sustain the cycle is higher for these materials. In Fig. 3.2 we illustrate the flame propagation:

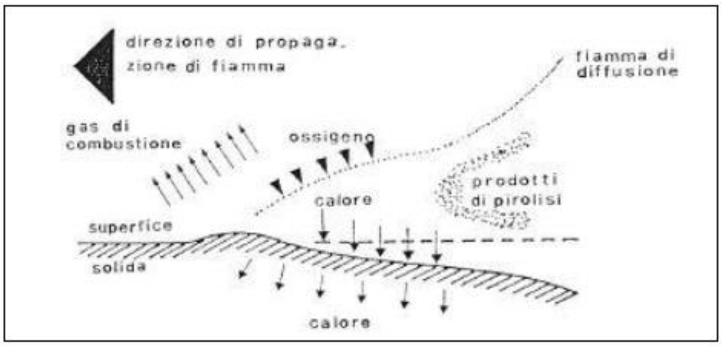

Fig. 3.2: *Schematic representation of propagation of the flame*

The mechanism of combustion is a free radical process, as we can see from Eq. 3.1 - 3.3, the propagation is highly exothermic:

$$HO^{\cdot} + CO \leftrightarrow CO_2 + H^{\cdot} \qquad (Eq. 3.1)$$

$$H^{\cdot} + O_2 \leftrightarrow OH^{\cdot} + O^{\cdot} \qquad (Eq. 3.2)$$

$$HO^{\cdot} + H^{\cdot} \rightarrow H_2O \qquad (Eq. 3.3)$$

Polymeric materials are highly inflammable, therefore **flame retardants** are required to spread their use also in sectors where the risk for fire is relevant. They must be stable at the melting temperature of the polymer and their smokes must be not corrosive or dark.

In general, flame retardants can slow down or stop combustion cycle of polymers. All of them can decrease the velocity of heat transferred to the polymer, reaching a value lower than the one required for the self-combustion. We can identify different mechanisms of action:

- *Halogen compounds*, as brominated and chlorinated additives, can inhibit propagation reactions of combustion by reacting with $OH^{\cdot}$ and $H^{\cdot}$**,** generating $X^{\cdot}$ radicals that are more stable; they act via chemical method by promoting termination reactions. Then, halogen acids are re-generated extracting hydrogen atoms from hydrocarbon species. Usually they are used at 10-20%.

  Their mechanism is indicated in Eq. 3.4 - Eq. 3.7:

$$HX + H^{\cdot} \rightarrow H_2 + X^{\cdot} \qquad (Eq. 3.4)$$

$$HX + OH^{\cdot} \rightarrow H_2O + X^{\cdot} \qquad (Eq. 3.5)$$

$$X^{\cdot} + RH \rightarrow R^{\cdot} + HX \qquad (Eq. 3.6)$$

$$X^{\cdot} + H^{\cdot} \leftrightarrow HX \qquad (Eq. 3.7)$$

- *Phosphorous derivatives* (DMPP, TCEP, etc.) that act on two fronts: they react with radicals inhibiting gas phase, and furthermore promoting char formation acting on solid phase. If condensate phase is promoted, few gaseous products are formed. Char formation does not permit the diffusion of volatile species to the surface generating a charred barrier that protects the underlying polymer and stops the thermo-oxidation of the polymer. For example, ammonium and melamine polyphosphates support char formation in polymer as polyamides, in addition to the dilution of vapor phase.

  In the condensate phase phosphoric compounds are converted in phosphoric and then metaphosphoric acid, which polymerises at high temperatures. With dehydration of the polymer carbonaceous layer is formed.

  Also inorganic compounds like silica or nanoclays inside the polymer promote generation of char, other co-additives favour reticulation of char, that in this way is more isolating. (Both chemical and physical actions are present).
- *Metallic inorganic hydroxides,* as trihydrate alumina ($Al_2O_3 \cdot 3H_2O$) or magnesium hydroxide ($Mg(OH)_2$), are characterised by endothermic decomposition, so they absorb heat, cooling the solid phase; since a cooling occurs, the burning velocity decreases. At T higher than 200°C alumina generates steam and, in addition, the products of these reactions dilute the products of the gas phase reducing the optic density; a further advantage is that gaseous species are not anymore within flammability limits. They act with a physical method.

  They are not corrosive, not expensive, but they should be used at high concentrations.
- Flame retardants that contain *expandable graphite*: when it is exposed to fire its volume increases by 100 times because of the expansion of its layered structure. So, the material becomes incandescent, but it does not burn (chemical method).

3.2 Evolution of flame retardants for polyamides

Now we focus on flame retardants for this group of thermoplastic polymers; thermic conductivity of polyamides is $0.23 - 0.27\ {}^{W}/_{K \cdot m}$, after burning they produce high amount of heat. Aramide textiles have flame retardant characteristics because of the aromatic structure, usually they are finished with other coatings to improve this property. We will focus on flame retardants for aliphatic polyamides, like Nylon 66, indicating the most common flame retardants and their features.

3.2.1 Chlorinated and brominated compounds

The most common chlorinated additive used for many years is a polycyclic polychlorinated compound, in combination with zinc borate allows lower smoke production and UV stability, but thermal stability is not satisfied [10].

One of the significant brominate additive for polyamides is decabromodiphenyl oxide, but for Nylon 66 negative aspects are discoloration and slight blooming; usually it is applied for textiles with a synergist, but other less expensive flame retardants are available, so it is not anymore commercially used. Alternatively, there are polymeric brominated flame retardants like brominated polystyrenes with higher thermal stability.

Nowadays they have been substituted because of environmental issue and another problem is that they are less effective for polyamides since, according to a study, hydrohalic acids that are formed cause chemical degradation of these synthetic polymers. A consequence is the decreasing of activation energy and the decomposition species do not change with bromo flame retardants [10].

3.2.2 Phosphorous compounds

Most important phosphorous flame retardants are red phosphorous, melamine polyphosphate, aluminium phosphonates; this typology of additives, as said before, act on both phases.

Red phosphorous, compared to other P-additives, resists to high temperatures and so it is perfectly appropriate for PA66 that has a high melting point; RP produces P_4 that later burns to give P_2O_5, it can enhance char formation. It can be used in combination with flame retardants based on nitrogen, therefore most efficient additives are those containing both phosphorous and nitrogen.

Aluminium diethylphosphonates can be used with *melamine polyphosphate*, indeed they have a synergistic behaviour for Nylon 66; the first one generates $PO^{\cdot}$ radicals acting on gas phase, instead the second one can work on condensate phase improving cross-linking between hetero atoms in amide groups. Another improvement can be obtained adding for example zinc borate, that enhance the formation of char barrier [1] for this polymer; flame retardants that can form strong bonds and increase cross-linking are necessary, for example three-dimensional structure from the polymerisation of metaphosphoric acid can be employed to retard the combustion of the polymer, shown in Fig. 3.3.

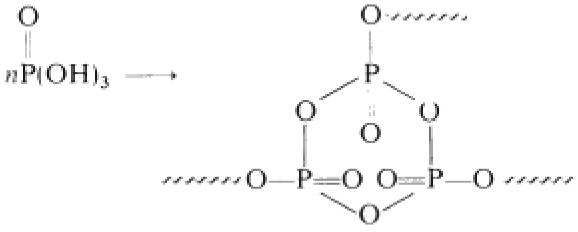

Fig. 3.3: *Polymerisation of metaphosphoric acid*

Alternatives to the previous examples without halogens or P are *glass fibres*, polymer cannot be damaged by heat thanks to expandable char formed on its surface. They behave like intumescent systems because they can increase in volume when exposed to temperature.

3.2.3 Textile finishing

The relevant problem connected to fire retardants for PA66 is the high processing temperature (above 280°C), indeed the majority of additives is not thermally stable. Moreover, they can reduce the strength of these fibres obtained by melt spinning. Monsanto and Solutia companies have proposed two solutions: the former a phosphine dicarboxylic acid, but it is too expensive, the latter a compound called Phosgard® that can add a phosphinate unit into Nylon structure, but it is still being developing.

To introduce flame retardants in the fabric different possibilities are available:

- *Reactive method or copolymerisation*: they react with molecular structure of the polymer becoming a permanent modification; the advantages are the durability of this treatment during washings and the homogeneity of the flame retardant in the material. It is more expensive and it is necessary to modify the synthesis process of the polymer;
- Use of compounds that are mixed with the polymer during polymerisation procedure;
- *Padding or spraying of an aqueous solution*: flame retardants are impregnated to polymer surface with a padder; in this case they have to be soluble in water or in alcohol because the textile with this procedure is dipped inside the solution.

3.2.4 Thiourea

For this work thiourea has been used to treat Nylon 66 textile, so in this paragraph we will provide some information about it.

According to literature review, thiourea (H_2NCSNH_2) has always been a proper flame retardant for Nylon, probably because of the synergistic effect of nitrogen and sulphur. Its use is appropriate for fabric coating, specially for fabric we are dealing with and cotton. It works by enhancing dripping in Nylon textile, by decreasing melt viscosity and the melting point of this polyamide. Usually this flame retardant is dissolved in water and applied using a laboratory pad mangle to eliminate the excess of the solution; then fabrics are dried in the oven.

According to DSC curve studied by Gilleo [9] the decomposition mechanism of Nylon changes after thiourea impregnation: an endothermic peak at 270°C occurs, this shows a reaction between Nylon and thiourea; he also observes an exothermic peak at 420°C occurs, it is not due to the decomposition of this flame retardant, indeed its decomposition temperature has not been defined; so it must be attributed to something different that is occurring in Nylon breakdown.

Therefore, thiourea is capable of promoting dripping and of modifying mechanism degradation as well, highlighting difficulty in understanding how it really acts on this polymer. Melting point of control Nylon 66 is 250°C, after applying thiourea it is around 200°C.

Different possible ways with which it acts are list here below [9]:

- Interaction with carboxylic groups;
- Reaction with amide groups;
- Nucleophilic attack by sulphur atom on polyamide bond;
- Deactivation of free radicals present in both phases;
- Reactions with species formed after homolytic cleavage in the condensed phase.

Now issues for human health and environmental safety regarding the use of thiourea are present, since it is a suspected carcinogen; it decomposes producing toxic fumes of nitrogen oxides and sulphur oxides, and it is toxic to aquatic organisms.

To improve **durability** of this treatment **formulations of thiourea-formaldehyde** are applicated to technical fabrics, treatment based on 1950-1980 chemistry. For Nylon finishing the structure of thiourea-formaldehyde oligomer with an acid catalyst is available to obtain a durable treatment because of the bonds between the amide groups of this polyamide and the finishing; its formula is $NH_2C(=S)NH[CH_2\text{-}NH\text{-}C(=S)NH]_nCH_2OH$. The reason why this mixture works is connected to the chemical processes that are involved, indeed cross-linking reactions are enhanced after its application. In Fig. 3.4 we represent the structure of urea-formaldehyde resin as flame retardant.

However, formaldehyde is a human cancerogenic compound, a highly reactive and flammable gas and it can react violently with other substances as acids. For these reasons its use should be avoided, when it is possible.

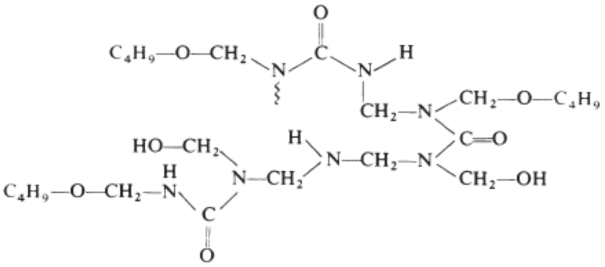

Fig. 3.4: *Urea-formaldehyde resin as flame retardant*

To conclude, we can say that in general inherently flame retardants have not been a success for polyamide fabrics, but only for aramids. Flame retardants must resist to PA66 processing temperature and be not dangerous for human and environmental health. Polyamides when heated show the inclination to gel and form cross-linking, but flame retardants are unsatisfactory [11]. Novel flame retardants and innovatory solutions to treat fibres must be found to guarantee good performances and costs, replacing formaldehyde-based structures.

Chapter 4

Instrumentation for the experiments

In this chapter we will analyse the four instruments that are used for the experimental part of this thesis: infrared spectroscopy in Fourier transformed FT-IR, thermogravic analysis TGA, LOI for flammability test, ultraviolet-visible spectroscopy UV-Vis and SEM machine. These tools are used to analyse PA 66 fabric after plasma treatment to determine what kind of changes are involved, and after soaking in thiourea solution to study the changes in flame retardancy. The objective is to comprehend if there are improvements compared to samples that are not exposed to plasma gas in the reaction chamber. Moreover, even if the polyamides are already hydrophilic polymers, another point of interest is the increase in wettability of Nylon 66 textile, reason why we perform also capillarity test. Hence, we will give the standard rules to study this aspect.

4.1 Infrared spectroscopy in Fourier Transformed (FT-IR)

This technique is based on the molecular absorption in infrared range (0.78-1000 μm), it is also called vibration spectroscopy: a molecule must have dipole moment to be visible with FT-IR, when molecules are exposed to infrared radiations, the energy given by the ray is converted in vibrational energy and molecular distance and bond angle vary thanks to this energy. Dipole moment μ changes (only with polar molecules), so the molecule vibrates and produce an electrical field. In Fig. 4.1 we illustrate all vibrations that can occur.

Bond vibrations can be listed here below, both can be symmetrical and asymmetrical:

- *Stretching:* elongation or shortening of molecular bonds; it is symmetrical if the same variations happen simultaneously, otherwise it is asymmetrical;

- *Bending:* deformations that can be on the plane (rocking and scissoring: angle modification) or out of the plane (wagging and twisting).

Degrees of freedom of a species with N atoms are 3N-5 for a linear molecule and 3N-6 for a non-linear one.

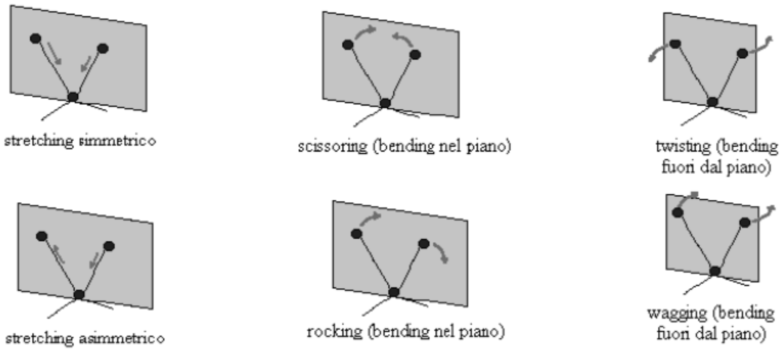

Fig. 4.1: *Bond variations*

Spectrum at wavenumbers lower than 1600 cm^{-1} is called the finger print region, here all characteristic absorptions for that molecule are present; instead for wavenumbers higher than 1600 cm^{-1} all functional groups are present at the same wavenumber, no matter what the structure of the molecule is.

Assuming vibration bonds behave as harmonic oscillator, we calculate vibration frequency with Eq. 4.1:

$$\nu = \frac{1}{2\pi c}\sqrt{\frac{k}{m}} \qquad (Eq. 4.1)$$

where ν is wave number [cm^{-1}], c light speed, k the constant of force [N/m] and m the reduced mass of the two atoms $\left[{m_1 \cdot m_2}/{m_1 + m_2}\right]$.

According to the model of quantum mechanics, only certain values of energy are allowed, ΔE is the right energy to provide to the molecule, so that it can jump to another energy level, bearing in mind that $\Delta E = h \cdot \nu$, where h is the Planck constant.

Thanks to FT-IR spectra both quantitative and qualitative analyses can be done: the former when spectra are registered in absorbance, using the Lambert-Beer law (Eq. 4.2) we can find concentration, instead the latter it is performed when spectra are in transmittance.

$$A = \varepsilon \cdot c \cdot \lambda = \ln\frac{I_0}{I} \qquad (Eq. 4.2)$$

where A is the absorbance, I_0 is the intensity of the radiation sent towards the sample, I the one emitted, ε coefficient of molar extinction, c the concentration and λ is the length of the optical path (the reciprocal of ν).

ε is constant for a substance at a precise λ. So, it is possible to calculate the concentration of that species after knowing its absorbance. Infrared radiations with frequency in the range 4000-400 cm^{-1} are sent to the sample and the spectra shows the absorbed peaks, from which we can understand what bonds are present.

Normalisation of peak area method is a way to calculate the normalised intensity of a specific peak to understand the amount of that functional group in the sample. The normalisation is considered with respect to a reference peak. Same peaks must be analysed using always the same coordinates of the region and of the baseline.

4.1.1 Working principle of the spectrometer

FTIR spectrometers are different from dispersive spectrometers, indeed they are based on Michelson Interferometer and they do not have monochromator; what we obtain is an interferogram, where intensity is plotted with time, then the Fourier Transformed calculates the plot source intensity - frequency. There are three mirrors: the fixed one, the moving one and the beamsplitter (in Fig. 4.2).

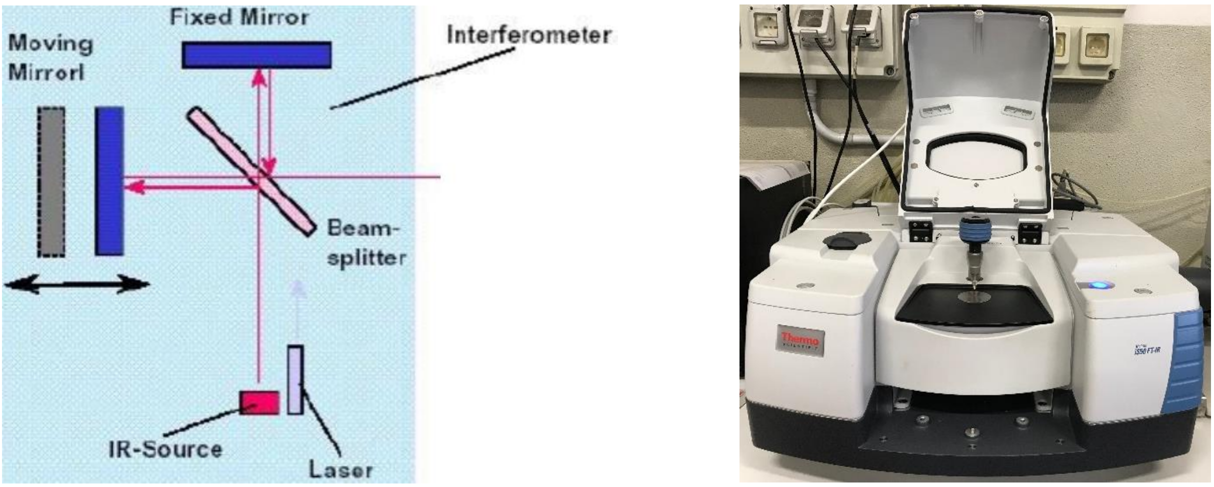

Fig. 4.2: *Scheme and equipment of FTIR spectrometer with Michelson interferometer*

The radiation is sent towards the beam-splitter, where it is divided in two parts thanks to the semi-transparent mirror: one goes to the moving mirror, the other one to the fixed mirror. Then after being recombined they are direct to the sample and to the detector, generating the interferogram. At the detector we have the intensity that varies with time, indeed time domain is connected to the position of the moving mirror (and so the transmittance of the sample). The interferometer converts the time domain into the frequency one.

Before collecting the spectra of the sample, it is necessary to collect the one referred to the background.

4.1.2 FTIR-ATR

Attenuated total reflectance technique is specially applied to solid samples, it is utilised for superficial analyses, for dark or with high thickness samples that cannot be characterised by IR spectroscopy in transmittance. The sample is pressed on the superior side of a crystal (ZnSe or GeSe). The radiation penetrates inside the sample for some angstrom, then there is a reflected component (it depends on degree of inclination) that goes towards the ATR crystal and after that it goes again towards the sample; this path is repeated many times. In Fig. 4.3 it is shown how this technique works.

If the sample is solid, it is positioned inside the instrument as a tablet with some KBr, for example, that does not absorb infrared radiation. It is necessary to mix some KBr with the interest material and then they are pressed at high pressure.

Also here spectra can be read either in absorbance or transmittance.

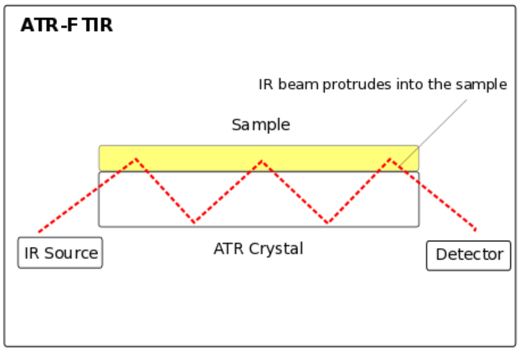

Fig. 4.3: *How ATR-FTIR works*

In Tab. 4.1 we report the wavenumber absorptions for the principal functional groups that can be found in FTIR spectra:

Tab. 4.1: *Characteristic absorptions in cm-1 for the most important functional groups*

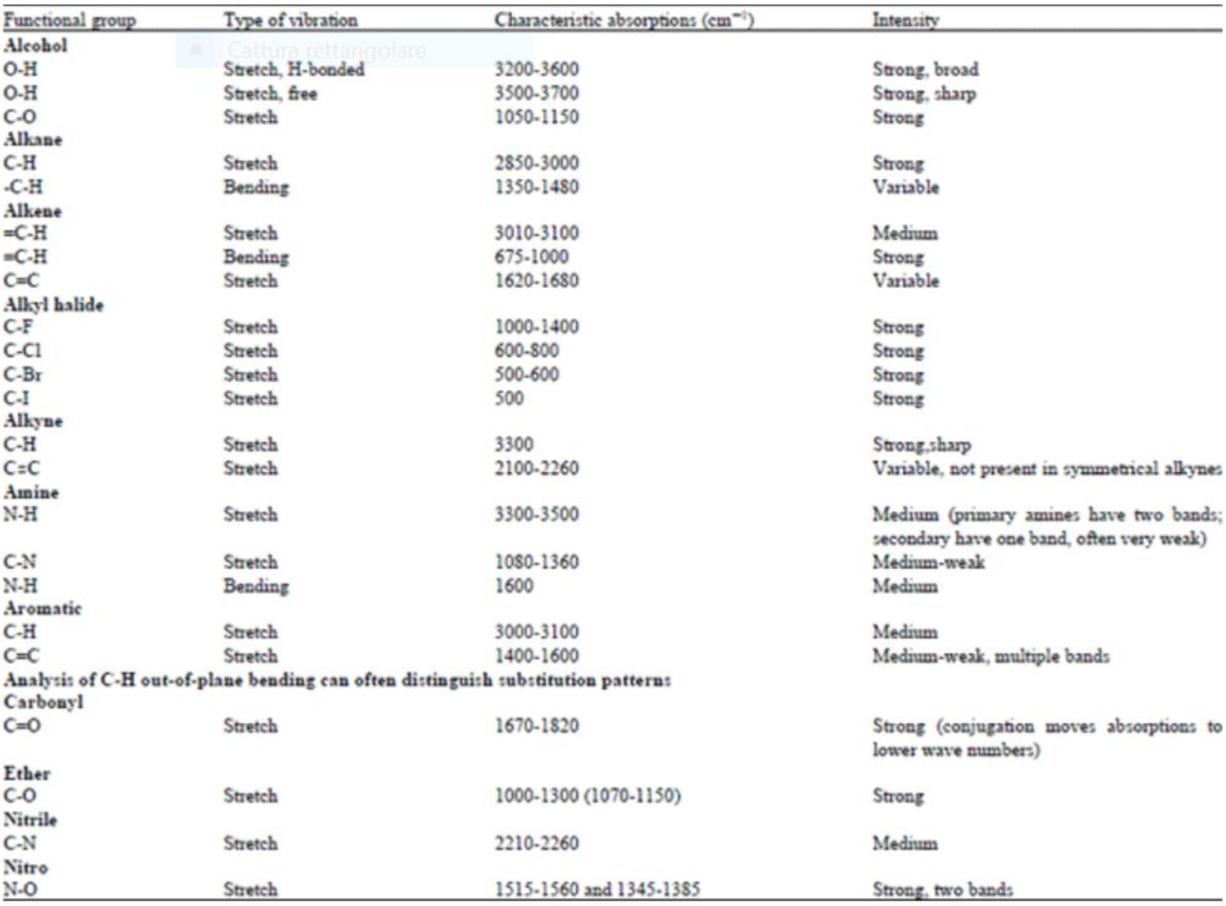

Functional group	Type of vibration	Characteristic absorptions (cm^{-1})	Intensity
Alcohol			
O-H	Stretch, H-bonded	3200-3600	Strong, broad
O-H	Stretch, free	3500-3700	Strong, sharp
C-O	Stretch	1050-1150	Strong
Alkane			
C-H	Stretch	2850-3000	Strong
-C-H	Bending	1350-1480	Variable
Alkene			
=C-H	Stretch	3010-3100	Medium
=C-H	Bending	675-1000	Strong
C=C	Stretch	1620-1680	Variable
Alkyl halide			
C-F	Stretch	1000-1400	Strong
C-Cl	Stretch	600-800	Strong
C-Br	Stretch	500-600	Strong
C-I	Stretch	500	Strong
Alkyne			
C-H	Stretch	3300	Strong,sharp
C≡C	Stretch	2100-2260	Variable, not present in symmetrical alkynes
Amine			
N-H	Stretch	3300-3500	Medium (primary amines have two bands; secondary have one band, often very weak)
C-N	Stretch	1080-1360	Medium-weak
N-H	Bending	1600	Medium
Aromatic			
C-H	Stretch	3000-3100	Medium
C=C	Stretch	1400-1600	Medium-weak, multiple bands
Analysis of C-H out-of-plane bending can often distinguish substitution patterns			
Carbonyl			
C=O	Stretch	1670-1820	Strong (conjugation moves absorptions to lower wave numbers)
Ether			
C-O	Stretch	1000-1300 (1070-1150)	Strong
Nitrile			
C-N	Stretch	2210-2260	Medium
Nitro			
N-O	Stretch	1515-1560 and 1345-1385	Strong, two bands

4.2 Thermal methods: thermogravimetric analysis (TGA)

The mass sample is recorded and it is plotted against temperature (thermogram) after a precise heating program; for this study we use SDT-Q600, TA Instruments, shown in Fig. 4.4.

Fig. 4.4: *SDT-Q600 TGA*

Inside the chamber two sensitive analytical balances are present, on these two alumina pans are positioned: one is empty and is the reference, instead inside the other one the sample (solid or liquid) is positioned, its mass is in the range 5-15 mg. We can run the experiment under nitrogen (inert atmosphere) or under air (oxidising atmosphere). From the computer heating rate and heating program are chosen; for the dynamic analysis we choose a certain heating rate, for the isothermal one instead the temperature is constant.

From the percent weight versus time, we can calculate for example the amount of organic and inorganic species inside the sample, the decomposition temperature, etc.

Depending on different factors the plot changes:

- Gas flow should not be too high to avoid problems for the degradation process;
- Mass of the sample: if it weights too much, the heat cannot diffuse homogeneously inside the material;
- Heating rate: we should avoid high heating rates because increasing this parameter also decomposition temperature raises, hence we obtain incorrected results.

4.3 LOI for flammability test

Many flammability tests are possible to evaluate performances of the studied material after fire exposure: UL 94 Vertical Flame Test, Cone Calorimeter, Hot Wire Index (UL 746C), Glow Wire Test, and finally Limiting Oxygen Index. Different criteria are adopted depending on the observed response: time of extinguishment, smoke formation, etc.

LOI test is performed to evaluate flammability behaviour of Nylon 66 according to ISO 4589-2 standard; the apparatus creates a mixture of oxygen and nitrogen with a constant flow rate of about 500 cm^3/s, the desired concentration is chosen by the operator. On the base a glass tube with open top is present, inside the textile material is kept in a metal clamp (80 mm by 15 cm). After the gas fills the cylinder, we perform the analysis. We should apply the flame for 30 s checking every 5 s if there is ignition [12].

LOI value is indicated in Eq. 4.3, units are in percentage:

$$LOI = \frac{100 \cdot O_2}{(O_2 + N_2)} \; [\%] \qquad (Eq. 4.3)$$

LOI is the minimum % volume of oxygen that can sustain combustion of that material under the conditions specified by the standards. O_2 and N_2 are in [cm^3/sec]. The equipment is shown in Fig. 4.5:

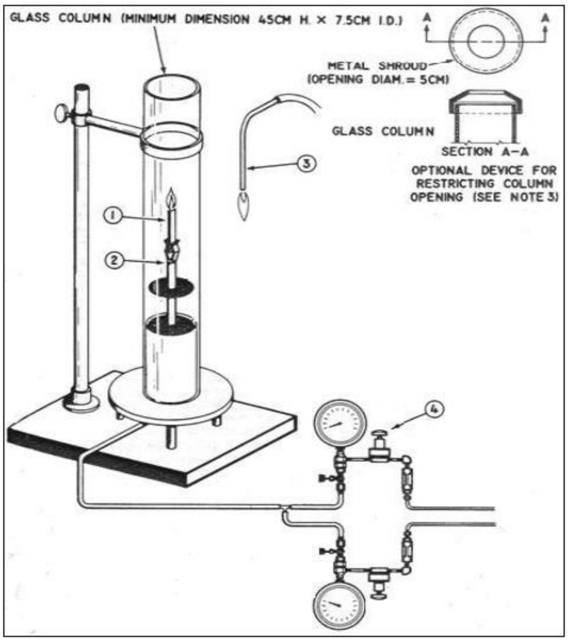

Fig. 4.5: Schematic *equipment for LOI test*

After the calibration, using propane gas we light the torch, then we start to perform several tests until the value is found, varying oxygen/nitrogen percentage.

The error of this equipment is ± 0.2.

Depending on this value, we can classify compounds in different categories: lower than 21% they are inflammable, if it is higher it means that the combustion does not occur in the atmospheric air. For flame retardants, values are greater than 27%. In Fig. 4.6 we represent LOI equipment with the textile holder used for this thesis.

Fig. 4.6: Laboratory *equipment for LOI test*

4.4 Ultraviolet-Visible spectroscopy (UV-Vis)

We perform this analysis with the Spectronic Camspec M501 in the visible light range 340-700 nm using a tungsten lamp (using the deuterium lamp the UV range 200-350 nm is emitted). This equipment is employed to carry out the DPPH treatment, that will be explained in chapter 5. The spectrum represents the trend of absorption as function of wavelength [nm]. In Fig. 4.7 we represent the equipment and a general scheme of a UV-Vis spectroscopy.

This technique uses the molecular absorbance, a group in the molecule that can absorbs the radiation is called *cromophore*; when atoms share electrons, from the linear combination of atomic orbitals we find the molecular ones. Absorptions deal with transitions from the ground state to the excited state, in a molecule the excitation of bond electrons is involved, so high energies are required. Different transitions are possible: $\sigma - \sigma^*$, $\pi - \pi^*$ (they are not possible between different symmetries). If the radiation is in the UV-Vis region, the electrons go to the excited electronic state, after that a band spectrum is obtained; in fact we have a lot of transitions (vibrational state are divided in rotational states), from a rotational state electrons pass to the upper one. Qualitative analysis is difficult to perform, but the quantitative one is very fast and cheap.

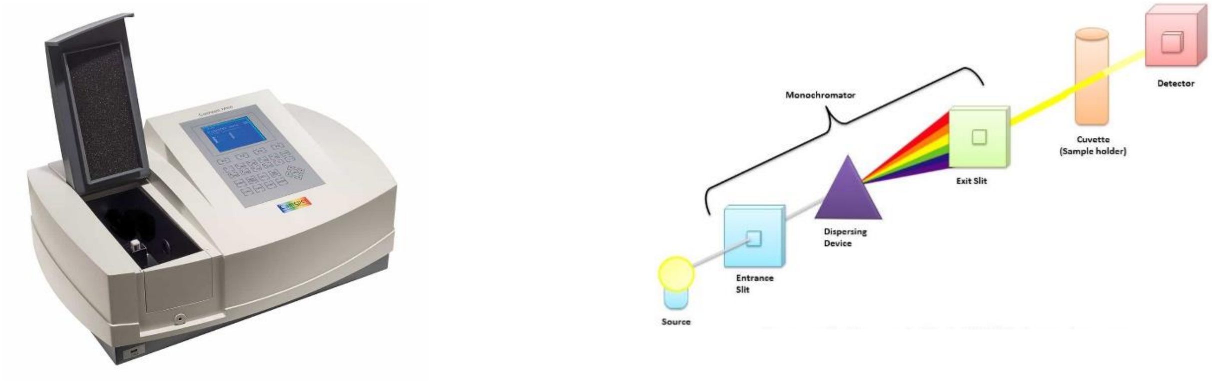

Fig. 4.7: *Spectronic Camspec M501 equipment and general scheme of the spectrometer*

The source generates a polychromatic beam, and it is followed by monochromator, which selects just one wavelength, after this hits the sample; the detector registers the corresponding absorption. The other wavelengths are instead dispersed.

Before registering the spectrum of the sample, the calibration is needed. At the beginning both of the cuvettes are filled with solvent (for example methanol) and we register this spectrum.

Then we start our analysis and in one of the cuvettes we put our solution, in the other one the solvent that was used for the calibration.

We define absorbance as $A = \ln\frac{1}{T}$, where T is the transmittance: $T = \frac{I}{I_0}$. I_0 is the intensity of the radiation that heat the sample, instead I is the intensity of the exit radiation from the cuvette; clearly $I < I_0$.

As described in § 4.1, also here Lambert Beer is valid: according to Eq. 4.4 absorption is proportionate to the concentration:

$$A = \alpha C_i l \qquad (Eq. 4.4)$$

Where α is coefficient of molar extinction that depends on the solution and the wavelength; C_i is the molar concentration of the sample, and l the geometrical length (the width of the cuvette).

4.5 Morphological characterisation: Scanning Electron Microscope

We perform some analyses using Hitachi S-3400N Scanning Electron Microscope (Fig. 4.8), since the objective is to characterise Nylon 66 morphology before and after plasma treatment. Previously, the samples are sputtered with a gold coating thanks to SC7620 Sputter Coater (Fig. 4.9), with a process current of 20 mA. The plasma current is variable adjusting the vacuum level using an Ar leak valve. We use 2 kV or 5kV as power of the electron beam inside the microscope.

Fig. 4.8: *Particulars of Hitachi S-3400N SEM*

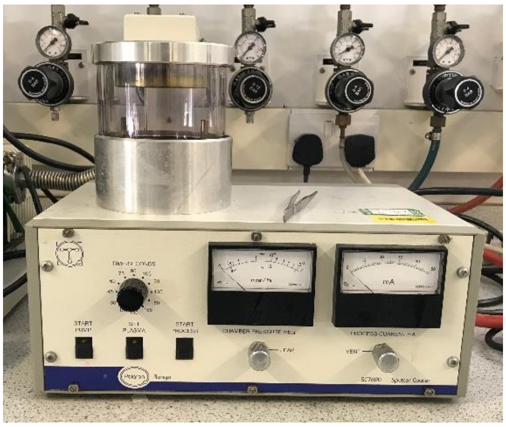

Fig. 4.9: *Sputter Coater*

This technique was invented by Ernst Ruska and Max Knoll in 1931 and improved by Hans and Zacharias Janssen in 1935.

It does not exploit the light as source of radiation, like an optical microscopy, but a beam of electrons. Thanks to magnetic lenses this beam is accelerated, it is focalized on the sample with different scans. In Fig. 4.10 a schematic representation of SEM is shown.

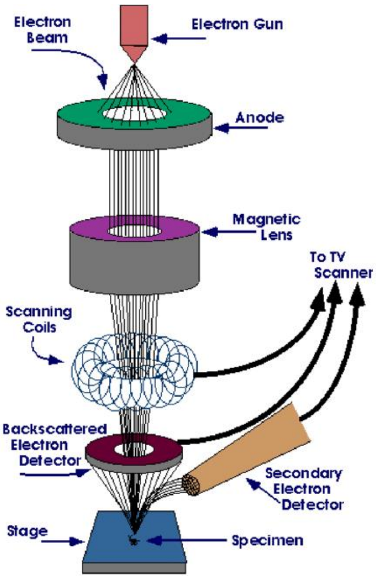

Fig. 4.10: *Schematic representation of SEM*

It is divided in various apparatus:

- Electronic column where the electron beam is generated;
- Vacuum chamber where we put the sample and the interaction between the sample and the electrons takes place;
- Different detectors that transfer to the computer the acquired signals;

- A screen to watch sample images.

Samples inside the chamber are very small and they have to fit on the specimen stage by using a conductive adhesive.

From this technique we can understand morphological information, in addition the structure and the composition of the sample. Secondary electrons are emitted by inelastic scattering interactions with beam electrons. They are originated at a depth of about 10 nm, after being accelerated their signals are sent to a multiplier, output signal can be viewed as a digital image.

4.6 Capillarity test

After plasma treatment a way to assess the change occurred on Nylon 66 textile is to perform wettability measurements using a solution of distilled water with a drop of ink. Nylon strips are dipped inside the solution with the lower end, holding vertically the material during the experiment. Stripes have a length of 10 cm and a width of 4 cm.

To evaluate wicking behavior of textiles we measure the height of capillary rise that occurs in a fixed time, or the time to reach a selected mark [13]. We decide to read the height after 6 min.

In the case of Nylon fabric it is not possible to evaluate the change in hydrophilicity with contact angles measurements, since the material is absorbent and the water drop disappears on the surface very quickly.

In chapter 5 we will evaluate this performance as function of the gas used and the power of the vacuum plasma.

Chapter 5

Experiments performed with atmospheric and vacuum plasma equipment

In this chapter we explain how we treated nylon fabric with atmospheric plasma (with the equipment present in the Fire Laboratory at the University of Bolton), followed by three analyses: SEM analysis, to see if any morphological change occurs, DPPH treatment, to understand if radicals were formed on the surface, and FTIR spectroscopy, to analyse the intensity peaks of some functional groups.

Besides, we focus on the processing with the vacuum plasma equipment at University of Padova, whose principles are explained in § 2.2.1. Here we show the optimisation of the process parameters to obtain the best treatment for nylon textile to maximise the functionalisation. We exploit FTIR spectra and the capillarity test to understand if it is possible to increase activation of Nylon surface.

Nylon used for this thesis was purchased from Aquafil S.P.A, whose area density is of 149.6 g/cm^2. The fabric exposed to plasma and flame retardant treatment has always been washed before treatment: the scouring is obtained soaking the textile in a 1% Triton X-100 detergent solution at 90°C for 1 h, and to follow the fabrics are dried in the oven at 70-80°C for 2 hours.

The first point of the study concerns textile treatment with plasma, but the final purpose is to add a flame retardant and understand which improvements on fire performances can be achieved introducing the plasma technique; so the second step will deal with the addition of thiourea to the textile, and with LOI test we will assess if flame retardancy properties improve after plasma treatment.

5.1 Atmospheric plasma treatment

We perform plasma treatment on Nylon 66 textile. The operative parameters used with torch plasma Microwave Power Supply SAIREM (§ 2.2.1) are reported in Tab. 5.1, and in Fig. 5.1 we see where the fabric is collocated. The ionized gases used are Ar and a mixture Ar/O_2 with a ratio equal to 4:1.

Observing the image below (Fig. 5.1) we can immediately say that this torch can cover only very small pieces of fabric, otherwise we should move the fabric on the wood support to allow the flame to pass over the all piece, leading to a non-homogeneous treatment. Therefore, we cut textile into pieces with a length of 10 cm and a width of 2.5 cm and we treat them forward and backward for 10 and 50 times, to understand what kind of changes affects the textile.

Tab. 5.1: *Operative parameters used with atmospheric plasma*

Scan speed	1.25 cm/s
Applied power	300 W
Length of the flame	2 cm
Distance from the fabric to the nozzle	5 cm
Diameter of the nozzle	0.5 cm
100% Ar flow	30 cc/min
Ar-oxygen gas	80% Ar - 20% O_2

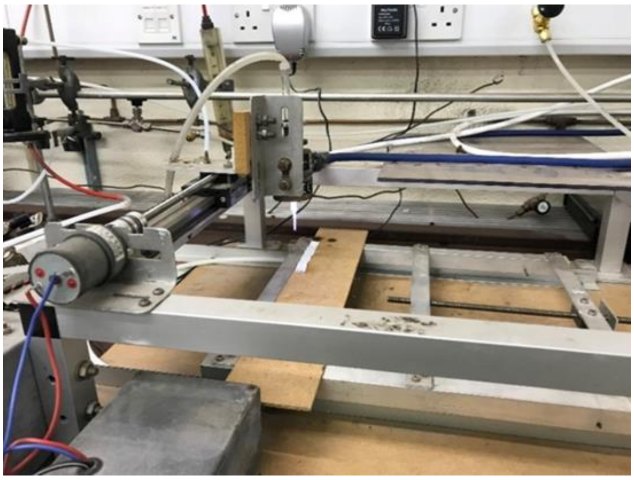

Fig. 5.1: *Nylon stripes treated with atmospheric plasma*

5.1.1 SEM analysis: morphological information

In Fig. 5.2 we show some images related to pure Nylon to obtain generic information about our textile, then the ones of the Nylon treated with Ar and Ar-oxygen plasma gases for 50 times.

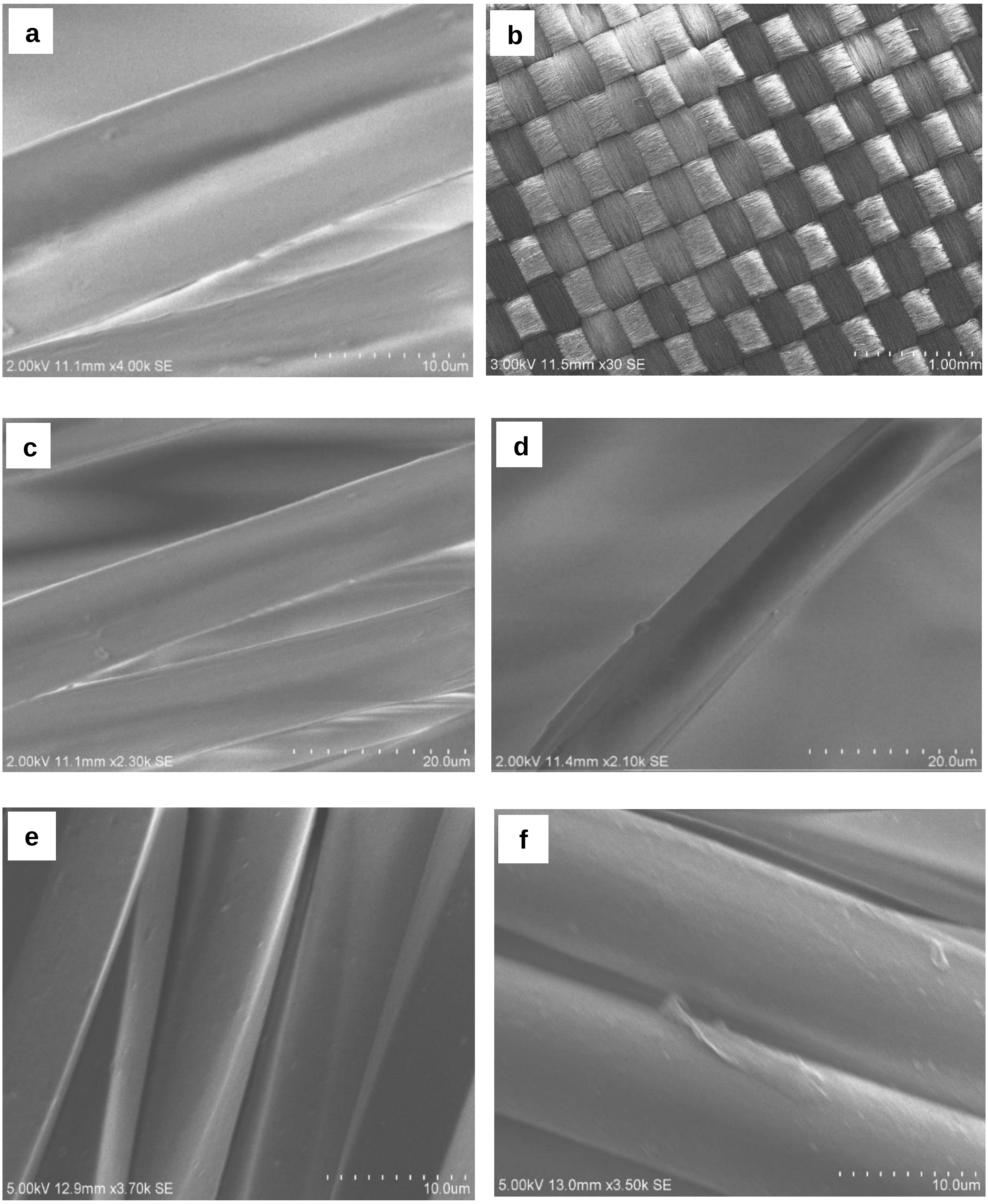

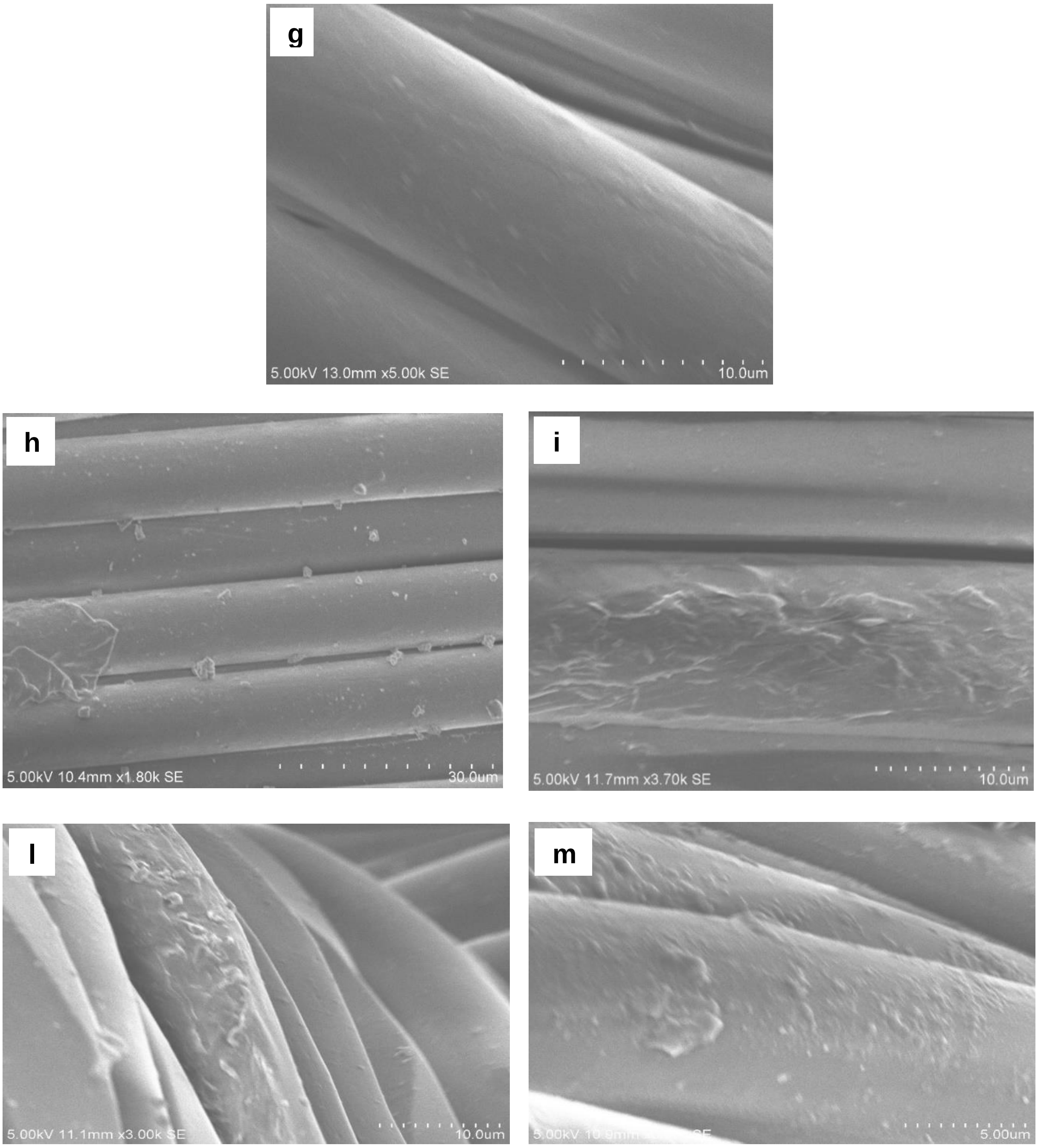

Fig. 5.2: (*a), (b), (c), (d) untreated Nylon; (e), (f), (g) Nylon after processing with Ar plasma; (h), (i), (l), (m) Nylon after processing with Ar-oxygen plasma*

From *a, b, c, d pictures* we can say that generally the fabric is a very tight, close sett weave; some fibers are circular in cross-section and some of them are square, so it can be that two different cross-sections are present or that heat setting during the textile production process (about 180°C) has deformed the fibres, indeed yarns are pushed close together. It is made by weaving yarns.

For Nylon treated with Ar plasma shown in *e, f, g pictures* we state that thanks to the peeling effect plasma starts to etch the immediate fibre surfaces. Ar-O_2 gas plasma has roughened fibre surfaces, as we can notice from *h, i, l, m images,* and further promote the release of surface coating species. Here we can see that probably scouring is not able to completely remove surface impurities present within the yarn structure, especially if this comprises a post finishing coating (nothing is specified by the company). We can notice modifications on the surface of the textile, small bubbles, some swelling and white spots, maybe because of the etching caused by the plasma.

P. S. Das, A. Bansode *et al.* report SEM images of Nylon 6 fabric after O_2, Ar plasma gases [14]; they notice that untreated film of Nylon is smooth, instead after Ar plasma treatment on the surface small globules appear, indicating an increase of surface etching. With O_2 plasma a higher amount of etching is seen, a more evident change in the morphology appears, producing globules with larger diameter; oxygen is indeed more reactive, as regards polymer surface. But in this case Nylon film is processed in vacuum condition (pressure of 10^{-3} mbar) with microwave assisted Electron Cyclotron Resonance plasma system; this is specific for surface modification of polymers. Instead our atmospheric plasma machine seems to be not able to introduce a significant morphological change.

In another study by C. Kan and W. Man on cotton textiles using an APPJ, Atomflo$^{\text{TM}}$ 400 machine for atmospheric pressure plasma treatment [8], using oxygen as reactive gas, at 130-140 W slits and grooves are present on the surface, and when power is 160-170 W the plasma is able to cause deep breakings, leading to etching; a surface-volume ratio is higher at these powers (Fig. 5.3).

Instead in our study, even at 300 W, modification is not so pronounced, revealing small effects.

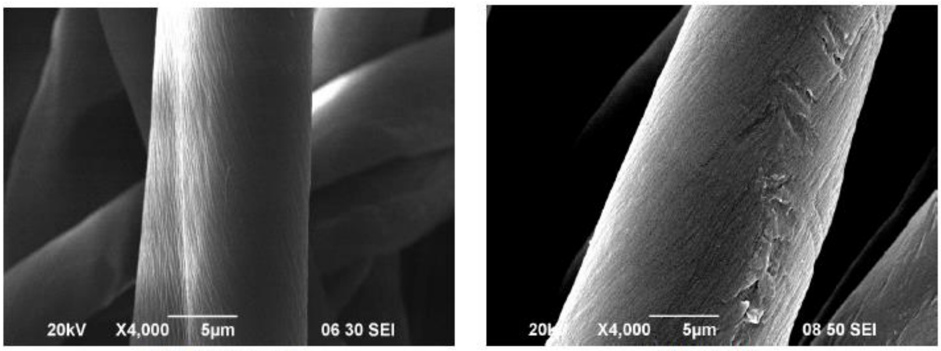

(a) Untreated (b) 130 W

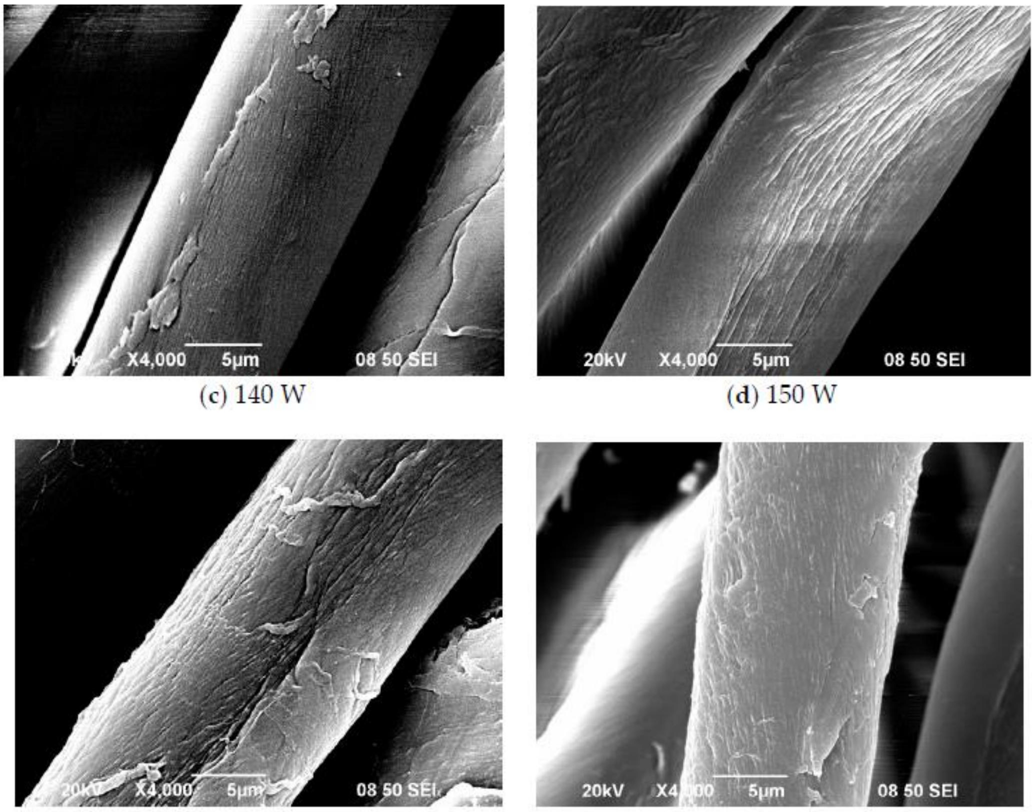

(c) 140 W (d) 150 W

(e) 160 W (f) 170 W

Fig. 5.3: *SEM images of cotton fabric treated with plasma machine mentioned above* [8]

5.1.2 DPPH treatment: Ultraviolet-Visible spectroscopy

First we want to explain what DPPH is and why it is used for this thesis; then we will report the results obtained with UV-Vis spectroscopy, in order to understand if radicals are present on Nylon surface after plasma treatment.

5.1.2.1 Objective of DPPH study

The purpose of this experiment is to understand if some radicals are present after plasma treatment. Thus, we are using a compound called *2,2-diphenyl-1-picrylhydrazyl*, which is a scavenger for other radicals. The DPPH radical absorbs at 520 nm and at around 350 nm, so it has a deep violet color in solution; instead it becomes colorless or pale yellow when it is neutralised. Therefore, from the change in the optical absorption we can highlight the presence of radicals on the textiles that are going to react with DPPH [15].

The DPPH used for these experiments has a characteristic absorbance of 0.861 at 517 nm and at a concentration of 100µM.

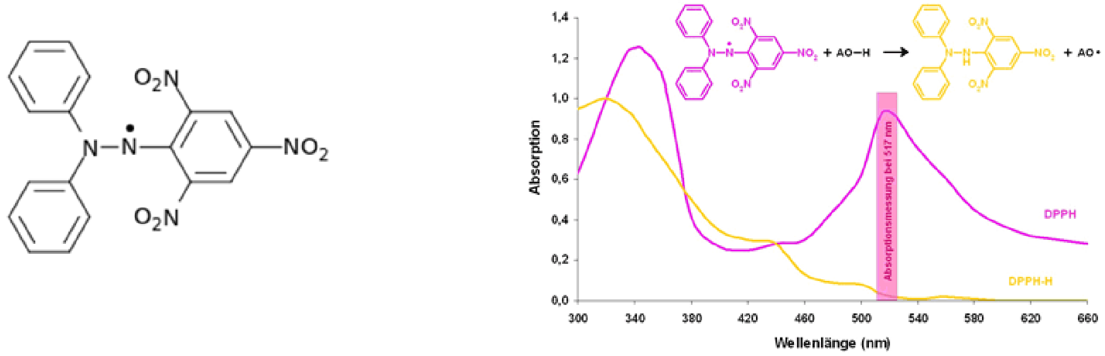

Fig. 5.4: *2,2-diphenyl-1-picrylhydrazyl structure and Absorption of DPPH and neutralized DPPH*

E. Hristea *et al.* investigate reaction of DPPH with $OH^{\cdot}$, $O_2^{\cdot -}$, HO$^-$, anions and other radicals and they detect with absorption spectra and thin layer chromatography the products [15]. They observe for example the formation of hydroxy-DPPH-H or its oxidation product (Fig. 5.5 and Fig. 5.6).

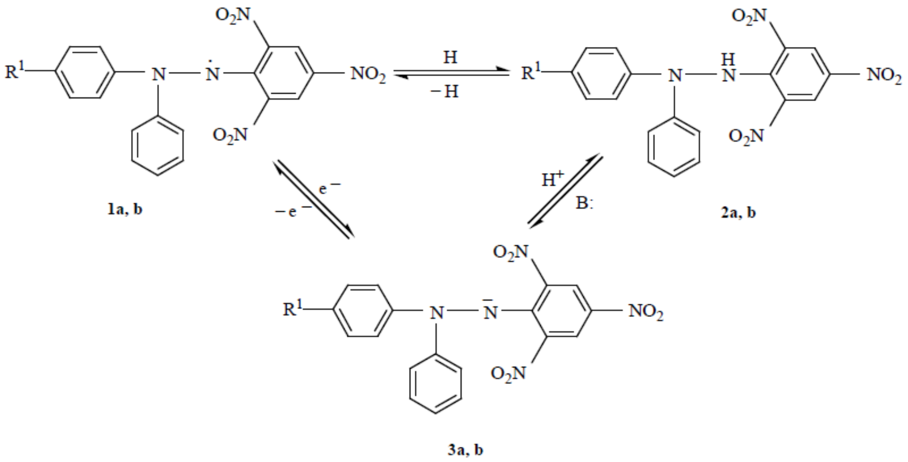

Fig. 5.5: Reactions of *1a (DPPH), 2a (DPPH-H) and 3a (DPPH$^-$)*

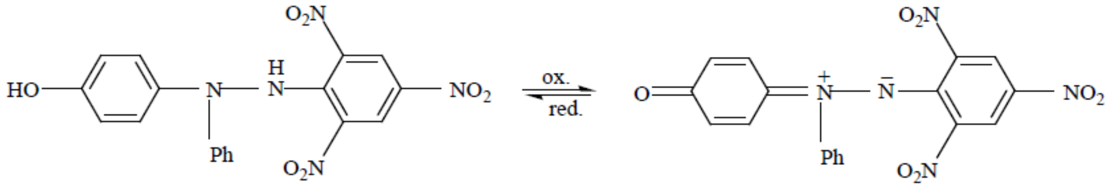

Fig. 5.6: *Redox reaction involving 4-hydroxy-DPPH-H and its oxidized product*

Reactions are rather difficult to understand, probably protolytic equilibria and redox processes are involved, in addition to molecular fragmentations.

5.1.2.2 Procedure and materials

We prepare a solution of DPPH of 100μM in methanol in the glovebox under nitrogen atmosphere (Fig. 5.7); the glovebox is a container where the operator can manipulate compounds using long gloves, avoiding the contact with the surrounding atmosphere. We introduce the materials through a system of double seals.

We pour 10 ml of the solution into five different holders, in each of them we dip a piece of pure nylon or one of the four treated samples (2 cm by 2 cm). All the holders are covered with aluminum foil to protect the sample from light and oxygen since DPPH is a stable radical, but it is sensitive to some solvents, oxygen, some Lewis basis, pH of the solution and light [16]. Indeed, B. Ozcelik *et al.* put DPPH in acetone or methanol solutions and keep the bottles under light source or enveloped with aluminum foil to see the differences in absorption at 517 nm. They show also the oxygen effect, both under dark and light conditions.

The stability of DPPH in methanol is higher than acetone, so this is the reason why we opt for this solvent. The absorption of DPPH in methanol decreases by 20% under light after 120 min, probably because photochemical decomposition occurs in presence of a light source. Sample with 21% presence of oxygen under light is causing DPPH absorption to decrease significantly. These effects are pronounced after 150 min, and, in general, the lowering of the absorption is more evident with time.

Fig. 5.7: *Glovebox under nitrogen to prepare DPPH solution and to preserve the cuvettes*

Before running UV-Vis spectroscopy we keep the cuvette under nitrogen, all of them under the same conditions, then we analyse them in the visible light range 340-700 nm using a tungsten lamp (using the equipment described in § 4.4).

5.1.2.3 Spectra results

Here below we show the UV-visible spectra for all the treated samples, the pure Nylon and the DPPH, as well. We examine the solutions after different time from the dipping of the piece: 15 min, 30 min, 1 hour, 1 and 2 days. In Fig. 5.8 we illustrate spectra of Nylon treated with Ar for both 10 and 50 times (Ar 10 and Ar 50 samples, respectively) backwards and forwards.

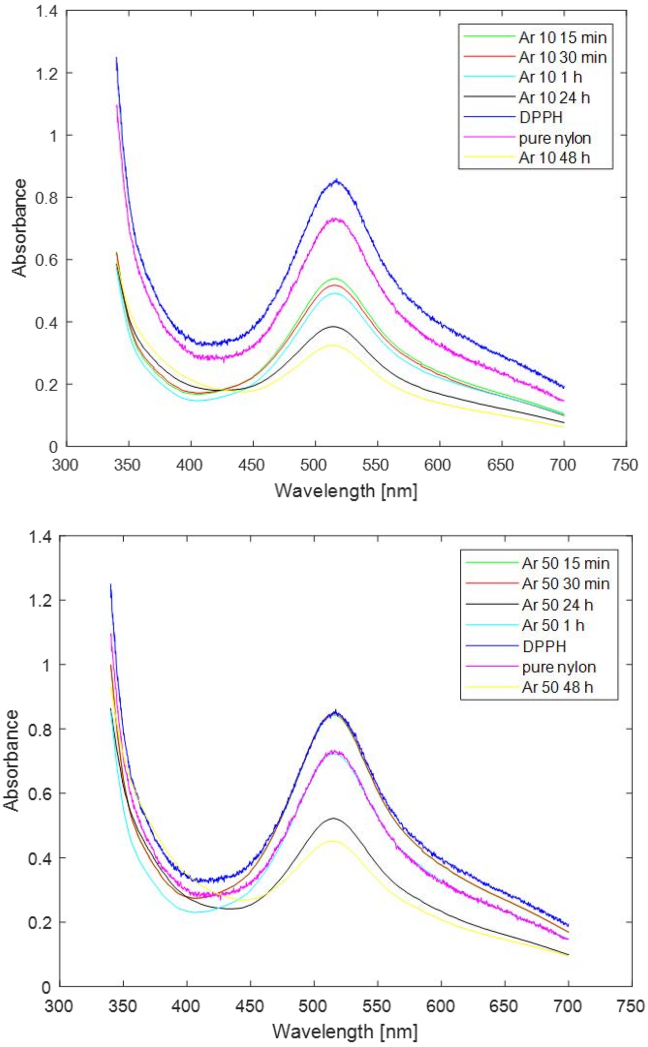

Fig. 5.8: *Spectra after Ar gas plasma*

Over time the absorbance is decreasing, so we notice that the radicals are still active even after one hour; obviously, the absorbance is much lower than the one of pure DPPH.

For Ar 50 treatment we see that treated samples after 15 and 30 min are overlapped with DPPH spectrum, showing no radicals. Instead we can notice that the trend of the pure nylon is not like the one of the DPPH, it may also happen that DPPH is not a scavenger only for radicals, but also for protons. Probably sometimes DPPH reacts with H- of NH- bonds, forming the compound DPPH-H.
But for the treated specimens after 1 h, 24 h and 48 h the absorbance is decreased.
We can conclude that maybe plasma becomes more effective after some time, at the beginning radicals seem to be more stable and the reactions involving radicals and DPPH could take place after one day.

The spectra related to the various samples treated with Ar-oxygen plasma are reported in Fig. 5.9:

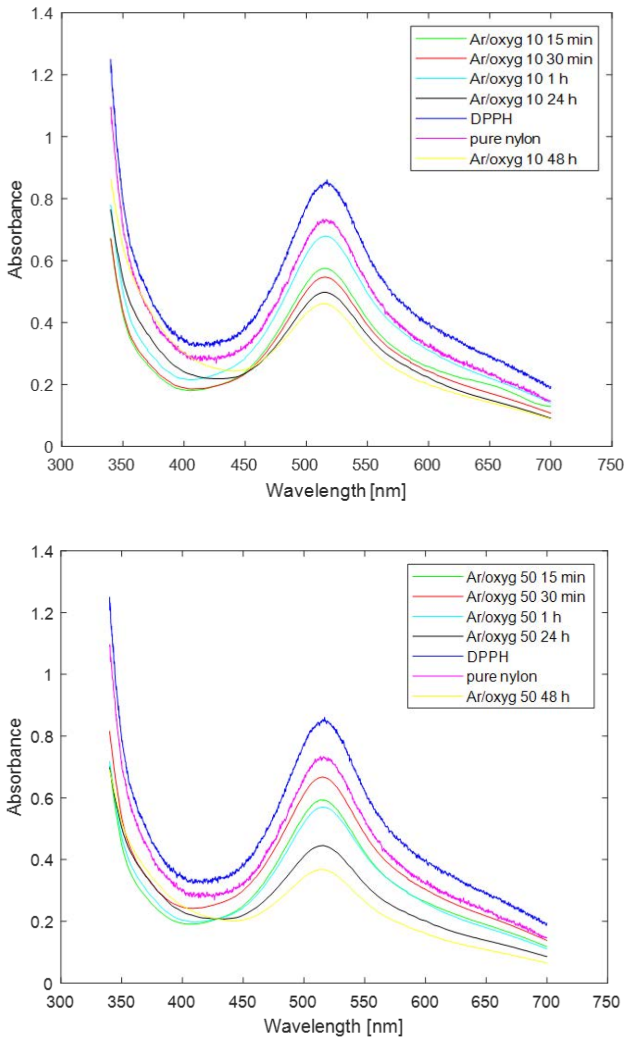

Fig. 5.9: *Spectra after Ar-oxygen gas plasma*

From Fig. 5.9 (10 scans treatment) we notice that the absorbance after 1 h is higher than the one after 15 and 30 min. Maybe more radicals are present after 1 h and they don’t react with DPPH causing cross-linkings, due to a quick mopping up; after one and two days maybe these weak bonds are broken and the radicals react with DPPH, involving photo-regeneration.

For the Ar/O_2 50 scans process we can notice that the absorbance decreases with time. This means that the radicals are still active. From Fig. 5.9 we state that the peak in the 500-550 region after 30 min is higher than the one of 15 min, maybe a sudden increase of radicals occurs after 15 min, which then react with DPPH, causing a decrease of the absorbance.

We conclude that with this technique it is not possible to understand what radicals are formed on Nylon surface, but it is only a qualitative way to have an idea of what it is happening. Certainly this experiment is not fully reproducible, and experimental errors occur during the preparation and analysis of the samples (like the size of the samples dipped into the DPPH solution, the non-uniform plasma treatment, the light and oxygen from the environment). Anyway, all the solutions are kept under the same conditions, if differences in absorption at 517 nm can be noticed between the solution where pure Nylon is present and the one where treated Nylon is dipped, it means that for sure radicals are formed on the surface after plasma technique.

5.1.3 FT-IR Spectra results

In this paragraph we show in Fig. 5.10 FTIR spectrum for Nylon 66 fabric, using the instrument described in § 4.1. In Tab. 5.2 we specify the wavenumbers of the main peaks [17].

Tab. 5.2: *Wavenumbers of the peaks analysed with FTIR*

WAVENUMBERS [CM^{-1}]	ASSIGNMENT
3295	N-H stretching
2932	C-H stretching (reference peak)
1633	C=O stretching (amidic band I)
1532	N-H bending (amidic band II)
1480-1300	C-H bending

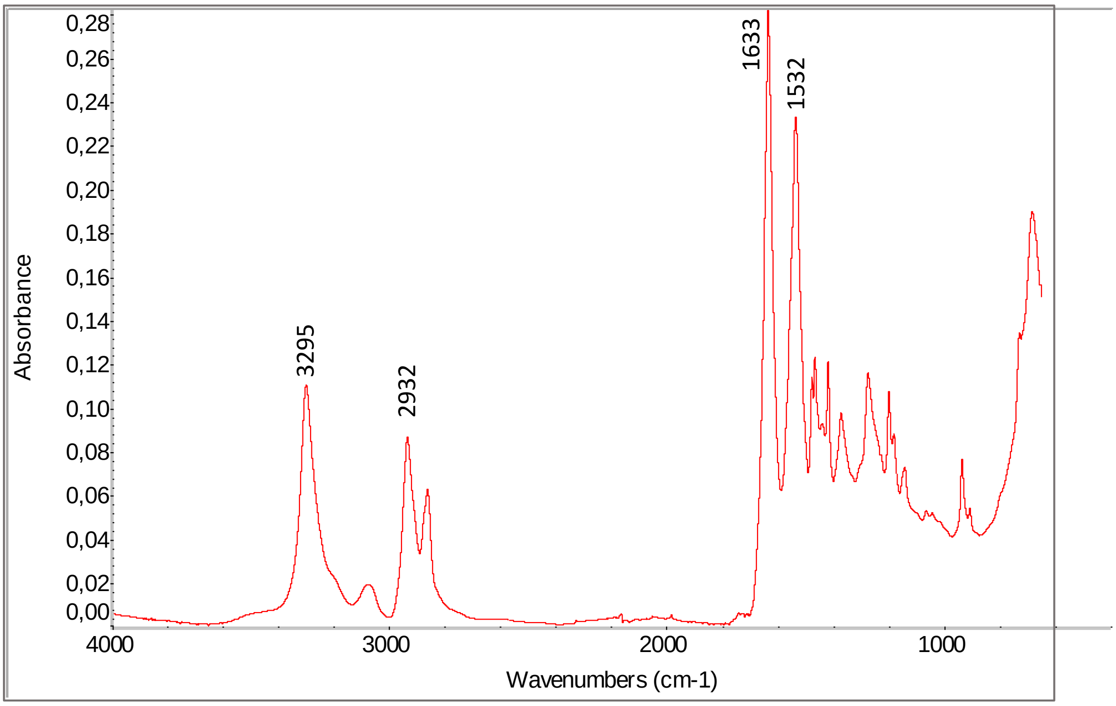

Fig. 5.10: *FTIR spectrum of Nylon 66*

5.1.3.1 Peak area normalisation

Using the *peak area tool* in FTIR software we analyse the area below some peaks, to see variation in the content of some functional groups after plasma treatment happens. Although the spectra are obtained by ATR, and therefore the optical path is almost constant, we prefer to normalize the results by using as reference peak the C-H stretching [18], i.e. a group which is not affected by the plasma treatment and which content is constant in treated and untreated samples. We will focus on the absorption peaks of $-NH_2$, -CONH- and -NH, indeed after atmospheric plasma oxygen can react with radicals formed on the surface to lead to the formation of -COOH groups, contributing to incorporate oxygen functionalities on surfaces; also amide groups can be formed [18], [19]. In order to analyse the surface in two different point (at the center of the sample, and laterally, 1.5 cm from the edge of the fabric), we cut a piece of nylon of 12 cm by 13 cm, the same size of the sample that will be treated with vacuum plasma. So it will be possible the comparison between the two different treatments. The FTIR analysis is carried out immediately after the plasma treatment.

Now we treat the textile for a fixed time, instead of deciding the number of paths; we choose 2, 5 and 10 min, moving the textile using the wood support and allowing the torch to cover the majority of Nylon surface. In Fig. 5.11 we show the trend of the normalised peak area (NPA) of three different functional groups as function of time for the fabrics treated with **Ar** and **Ar-O_2 gas plasma** and for the one of pure Nylon (control sample) as well, to compare all the values.

As expecting, this treatment is not homogeneous, indeed there are significant differences between plots taken from the centre of the sample and its edge; the disadvantage of this equipment is that it is not possible to process at the same time all the fabric, the flame can afford only a local treatment and, moving manually the wood support, we cannot generate a uniform activation on the all fabric. Moreover, for CONH- group, values for both gases of treated specimen are lower than the ones of the control sample (either at the centre or at the edge), this means that this plasma is causing probably breakings, etching, and it is not instead increasing absorption peaks of this functional groups.

Introducing oxygen gas during the processing seems to not improve the textile treatment, also for the NH_2- group at the center of the specimen NPA value at 2 min is even lower than the one referred to the pure specimen.

In general we can say that this plasma equipment promote a limited activation of Nylon 66 textile; moreover, the treatment is not uniform at all, so it makes no sense to proceed with flame retardant treatment.

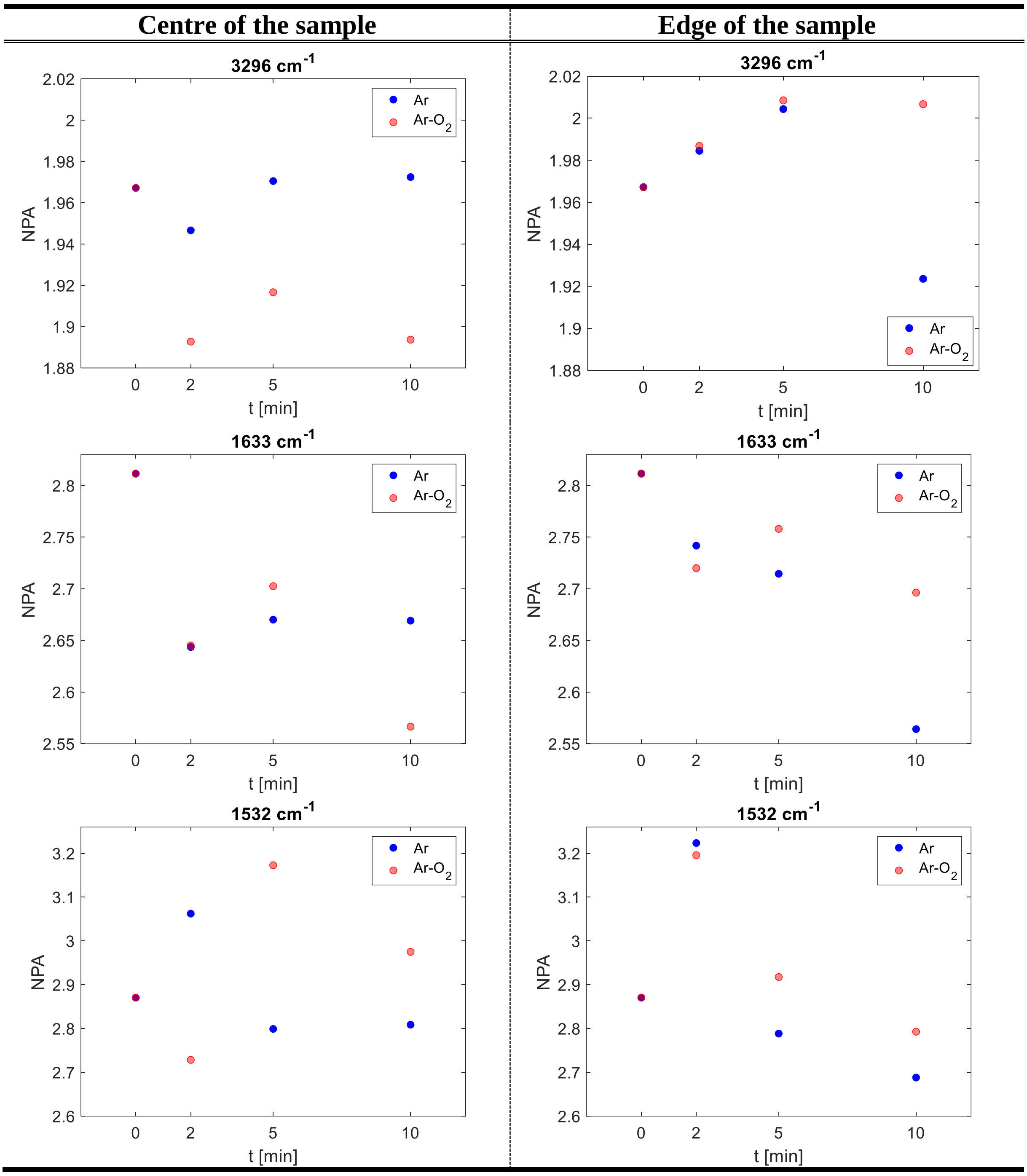

Fig. 5.11: *Normalised peak area at the centre and at the edge of the sample for NH_2-, CONH-, NH- groups*

5.2 Functionalisation process and parameters for vacuum plasma

We put the fabric on a glass Petri dish, that will be placed inside the vacuum chamber of the reactor microwave Miniflow 200SS (Fig. 5.12), used as support of the material. We choose a precise distance from the surface and the torch, trying to minimise the distance, but at the same time avoiding any damage on Nylon fibres. For this purpose we use the Thermo Scientific Nicolet Centaurμs FT-IR Microscope (Contact Alert™), reported in Fig. 5.13, examining the sample with a Triton 10x Objective. The treated textile is a piece of 12 cm by 13 cm.

One of the main disadvantage of this equipment under vacuum is the size of the material that can be treated per batch since it is limited by the chamber dimensions; moreover, it is a batch system, so the productivity is not very high; finally, the use of vacuum equipment is much more expensive than atmospheric plasma.

Inside the chamber we create the vacuum first closing the gas leak valve, then slowly closing the high vacuum valve, and turning on the vacuum diaphragm pump, reaching about 6 mbar. Finally we switch on the turbomolecular pump, connected in series, to reach high degree of vacuum.

We regulate the flow of the gases entering the reactor thanks to digital flowmeters and we maintain the chosen pressure with a regulator valve, working on the total percentage of gas that is going inside the chamber. We see the % of total gas from FlowDDE (Bronkhorst®) server, that handles all communication data to the instruments. It allows an interprocess access between the computer and the digital flowmeters. From this software it is also possible to decide the exact flow rate of oxygen.

The functionalisation is then activated pressing the button *ON* present in the touchscreen when all the chosen conditions are reached.

Fig. 5.12: *Microwave Miniflow 200SS Plasma Equipment*

Fig. 5.13: *Thermo Scientific Microscope to observe Nylon fibres*

The goal of this technique is to see if flame performances, evaluated by LOI test, are increased, because of a higher amount of thiourea attached on the surface thanks to the activation of the surface and/or the formation of strong bonds between the flame retardant and the functional group generated on Nylon.

5.2.1 Fixed and variable parameters

Now we list the parameters that are kept constant during the various experiments:

- Pressure: we keep inside the chamber a value of about $6 \cdot 10^{-2}$ mbar. This reactor usually should work at a pressure of the order of 10^{-3} mbar, but we want to guarantee a total gas entering the reactor at least of 0.3-0.5% of the total volumetric flow entering the reactor, that is 30 cm^3/min. Indeed the flow is necessary for the activation, so we remain at higher pressure values.
- Distance from the torch: we set this parameter at 30 mm, finding a compromise between a better functionalisation of the textile being closer to the torch, and no damage on the fibres, observing the textile with the microscope after the treatment.

Instead the parameters that are changed for these studies are the following:

- Time of treatment: we decide to vary this parameter choosing 2, 5, 10 min, according to conditions performed in other experiments using vacuum plasma [19]. We evaluate the best time treatment using FTIR spectra evaluating the increase in the concentration of the functional groups mentioned in § 5.1.3. In this case we keep constant the power at 80 W.

- Power: maintaining fixed the time treatment, we modify power values: we set values between 40-200 W, with step of 40 W.
- Gas plasma: we carry out all these experiments using He/oxygen gas, so a mixture of the inert gas and the reactive gas; for a fixed time and power, we change the gas ratio (He/O_2 5:1, 1:1, 10:1). The benefits in terms of functionalization have been assessed by FTIR spectra and capillarity test. Trials using neat helium or oxygen have also been carried out.

  According to literature review [20], inert gas plasmas as Ar or He, can abstract hydrogen atoms from polymer chains, generating free radicals, clean the surface removing low MW species. Instead oxygen gas plasma can increase the presence of oxygen functional groups thanks to the reactions between the active molecules of the plasma and the molecules on the surface (as explained in § 2.3). So, usually, to have an increase of wettability and a stability of the treatment, a mixture of these two types of gases should be used.

5.2.2 Effect of He/O_2 ratio, power and time

To analyse which He/O_2 ratio guarantees a better functionalisation of PA66 textile we analyse FTIR spectra and perform the capillarity test. First we want to decide at which proportion we have to work, and then at which power and time.

5.2.2.1 He/O_2 volumetric ratio

In the following plots we show NPA values for the three peaks, as before, changing He/O_2 proportions: 1 to 1, 5 to 1, 10 to 1. We treat the fabric at 80 W and for 5 min. FTIR spectra at the center of the sample have been collected after plasma treatment. Moreover we add results of capillarity test for each of them, following the procedure explained in § 4.6. In Tab. 5.3 we report all the results.

For 10:1 ratio we obtain the worst results, with two values of NPA even lower that the corresponding ones of pure Nylon; we also notice the lowest value of liquid rise, NPA values for all the peaks are lower than the ones of the other two ratios, as well. We decide to proceed for all the future analyses with **5:1 ratio** since all NPA values, in particular the one related to CO-NH group, are higher, like also the capillarity rise.

Tab. 5.3: *Normalised peak area for the three functional groups and capillarity test at different volumetric ratios*

1 to 1

Wavenumbers [cm^{-1}]	NPA	height [cm]
3296	2.031	5.2 ± 0.34
1632	2.855	
1532	3.31	

5 to 1

Wavenumbers [cm^{-1}]	NPA	height [cm]
3296	2.156	5.5 ± 0.42
1632	3.054	
1532	3.429	

10 to 1

Wavenumbers [cm^{-1}]	NPA	height [cm]
3296	1.952	4.6 ± 0.47
1632	2.721	
1532	3.165	

Pure nylon

Wavenumbers [cm^{-1}]	NPA	height [cm]
3296	1.967	4.6 ± 0.43
1632	2.812	
1532	2.87	

5.2.2.2 Microwave source power

In this paragraph we represent the trend of NPA values for the three peaks as function of the power used to activate the plasma inside the chamber. For this experiment we treated the samples for a fixed time, 5 min. We collect the FTIR spectra at the centre of the sample for all the treated fabrics. In Fig. 5.15 we show these plots, instead in Fig. 5.14 we represent capillarity rise versus power, including the value related to the control sample to assess at which power is better to functionalise the textile.

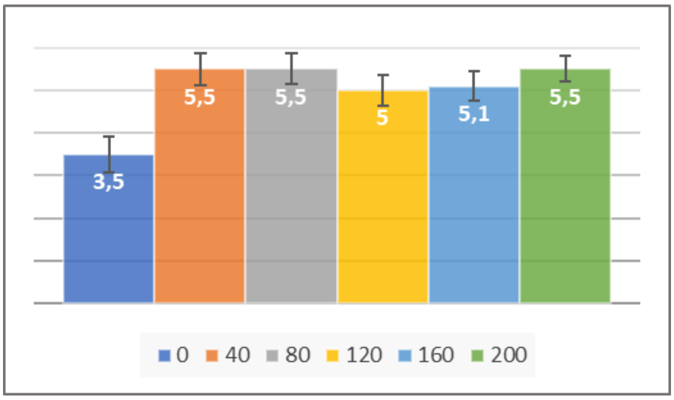

Fig. 5.14: *Capillarity height [cm] versus power [W]*

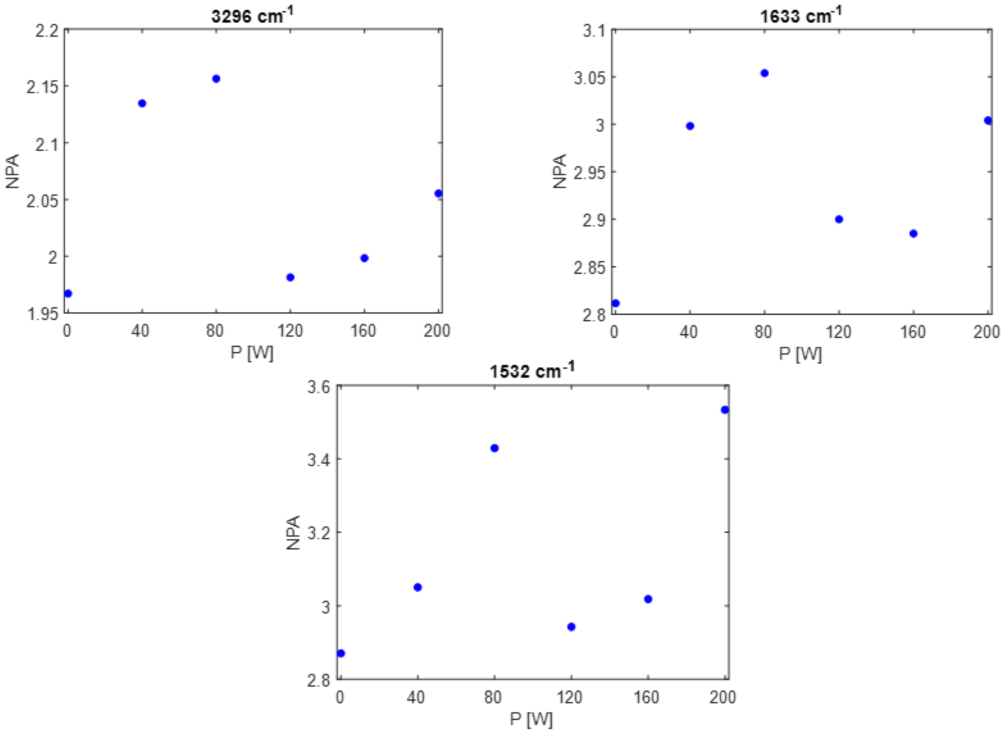

Fig. 5.15: *NPA values versus time for three different peaks*

From Fig. 5.15 it can be seen that vacuum plasma can produce a more efficient treatment at 80 W, since NPA values are higher for this experiment; from 0 to 80 W there is an increase in absorption for all three peaks, but at 120 W we observe a rapid decrease; from here up we notice again an increase up to 200 W.

About the wettability test we see the highest capillarity rise for 40, 50 and 200 W. Indeed, at these powers we have observed the higher values of NPA for both CONH and NH groups, and an increase of the polarity of the material is expected to increase the liquid absorption, and therefore the wicking height. Plasma process parameters like the power are relevant for the efficiency of the treatment. These two plots prove that when the absorption of, for example, carbonyl functional group increases, also hydrophilicity of the Nylon raises, thanks to surface oxidation [21].

For this equipment a power of 80 W is enough to obtain optimal hydrophilicity.

5.2.2.3 Treatment time

Another parameter that should be considered is the time; as we did for the atmospheric plasma device, we perform FTIR study either at the centre of the specimen or at the edge, to understand if this treatment can generate a homogeneous activation of the fabric. Now we change time to see how NPA values vary with this parameter.

From Fig. 5.16 we see that treating the Nylon inside the chamber of the vacuum reactor a uniform processing is allowed, the plasma torch is able to generate over the whole surface a similar increase of NH and CONH peak areas with respect to the control sample.

Considering NH bond, NPA values are approximately similar for the three different times, since all of them are around 2.15; instead for CONH bond 5 min is the best time treatment.

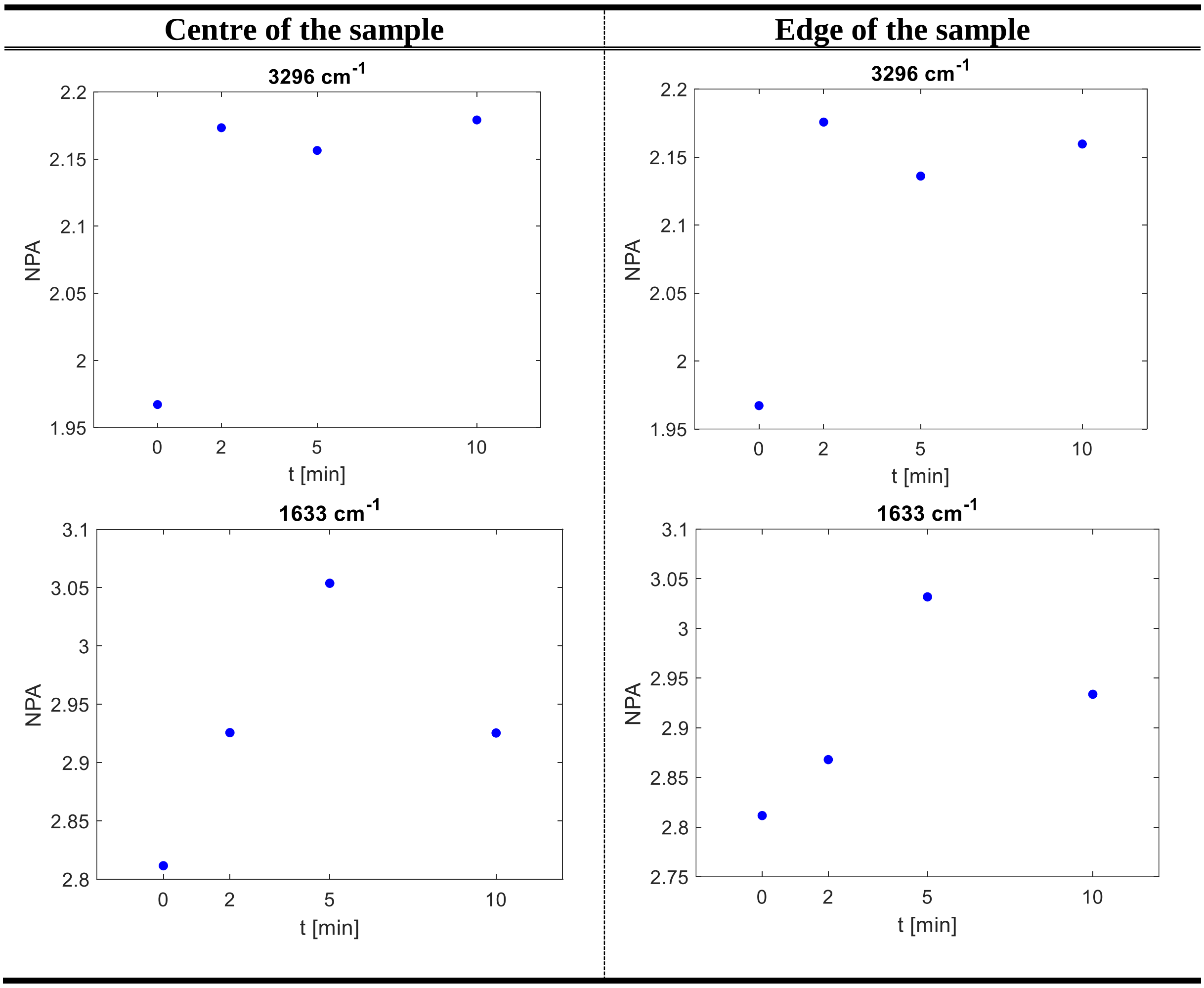

Fig. 5.16: *Normalised peak area at the centre and at the edge of the sample for* NH_2*-, CONH- groups*

To conclude, for the following studies about the addition of thiourea after plasma treatment and the LOI test we will select the following parameters: 80 W, 2 min, 5 to 1 for He/O_2 gases.

5.2.3 TGA results

We present in Fig. 5.17 the trend of weight loss versus temperature for pure Nylon and for Nylon after plasma treatment. We run the TGA experiments under air with heating rate of 20°C/min, until the temperature reaches 900°C. The error of the measure of the residue weight for this instrument is 1%. We calculate the extrapolated onset temperature, that is the temperature at which the weight loss begins (T_o), used by ASTM D 2863 and ISO 4589 [22].
We can observe two stages in the thermo-oxidative decomposition of Nylon: the first occurs between 350-480°C and the second above 480°C, where oxidation of the char happens. Most of the weight loss takes place in 400-500°C region. The thermal behavior between the two samples is the same, indeed the two curves are almost overlapped. For both curves we can assess that the T_o is around 425°C, with a total mass loss of more than 99.%.

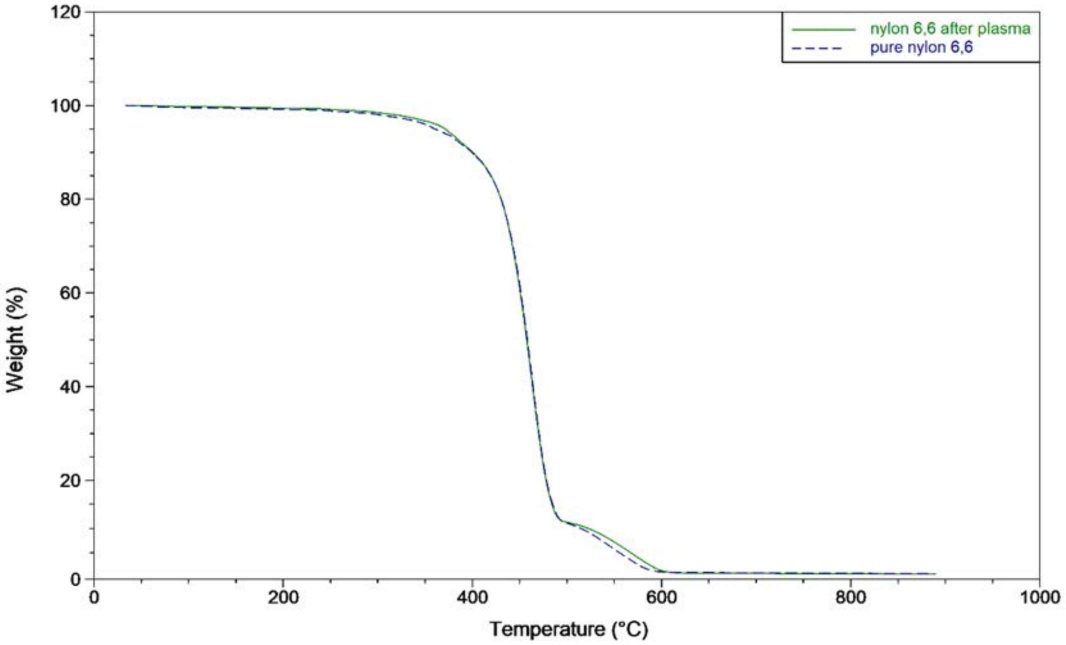

Fig. 5.17: *TGA plot for pure Nylon and Nylon after plasma process*

5.2.4 Impregnation in thiourea solution

After showing results of plasma processing, we move to the next step of this work: to understand if the application of thiourea on the fabric is favored by plasma activation.

We prepare a solution with distilled water and thiourea, so that we can achieve 80-90% of wet add on. We dip the fabric in the solution for 15 min (impregnation), and then we pad it twice using a pad mangle; the padder is made up of two horizontal rollers were the fabric is guided vertically (nipping) to squeeze the solution (Fig. 5.18); so, in total, we deal with two dippings and two nippings. Then the samples are dried in the oven at 70-80° [23].

The treated samples with ionized gas are dipped into the solution immediately after the treatment, so that we can maximise the add on % of the flame retardant.

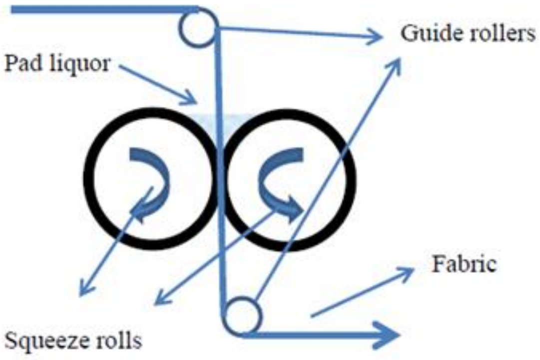

Fig.5.18: *Nipping through two rollers after dipping in thiourea solution*

We want to compare the untreated samples with specimens treated with He/O_2 gas; we use two methods to calculate the amount of flame retardant present on the fabric: the first one is the calculation of the dry add on % with Eq. 5.1 using Mettler AE 240 balance.

$$Dry\ add\ on\ \% = \frac{weight\ after\ dry - weight\ before\ FR\ application}{weight\ before\ FR\ application} \qquad (Eq. 5.1)$$

The second method instead deals with TGA equipment, using the instrument described in § 4.2. We show in Fig. 5.19 the trend of pure Nylon, pure thiourea, Nylon treated with plasma and thiourea (red curve) and Nylon treated with thiourea only (blue curve). Since thiourea loses most of its weight (around 80%) up to 330°C while nylon weight is almost constant, the amount of thiourea in treated samples can be calculated by considering the weight loss up to 330°C.

We observe immediately that at the same temperature (330°C) the sample processed with plasma loses more weight, so it contains more thiourea. We perform different runs with different samples to have the standard deviation values. Plasma conditions are mentioned earlier.

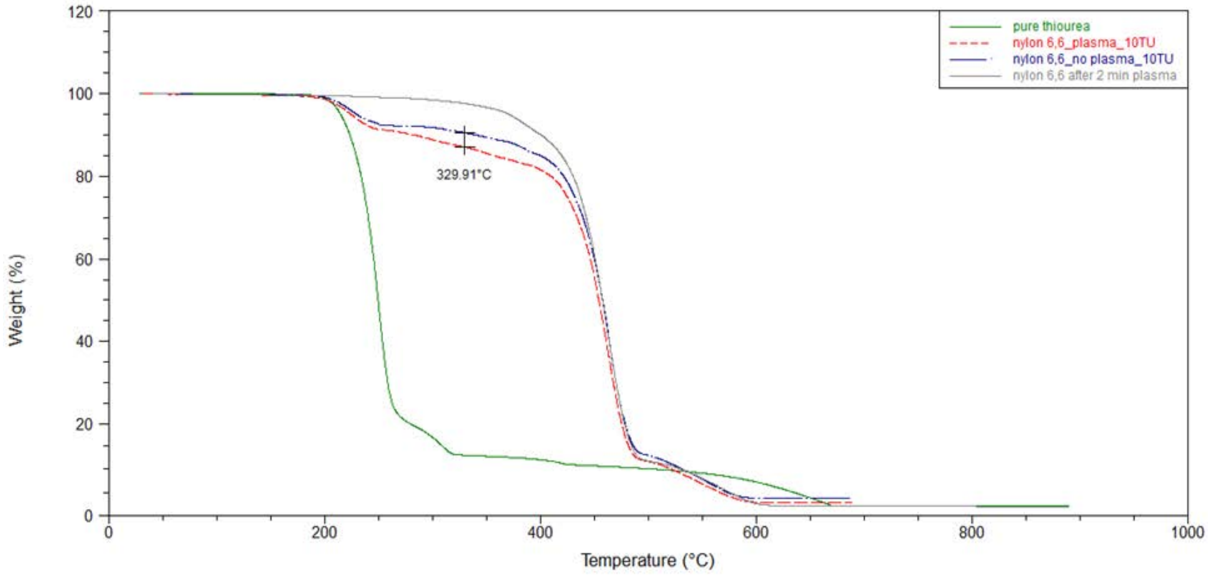

Fig. 5.19: *TGA plot to calculate thiourea amount on Nylon fabric*

We summarise in Tab. 5.4 dry add on values calculated either with the balance method or with TGA. In this case the solution has 10 mass/volume percentage of thiourea (thiourea is the solute, distilled water is the solvent).

Tab. 5.4: *Amount of thiourea present on Nylon textile for 10% thiourea in solution*

Dry add on [%]	TGA result [%]	
9.84 ± 0.06	8.9 ± 0.5	Nylon without plasma
11.18 ± 0.28	10.23 ± 0.4	Nylon after plasma

We see that more flame retardant is attached on Nylon fabric after He/O_2 gas plasma, this should lead to an increase of flame retardant properties. For the following concentrations we prefer to measure the amount of flame retardant present on the fabric with the balance since this method is less time-consuming and allows to obtain a more representative value of the whole sample, because of the higher dimension of the sample used for the determination.

Tab. 5.5: *Amount of thiourea present on Nylon textile for different solution concentrations.*

	Pure nylon	Plasma Nylon
5%	4.15 ± 0.39	5.51 ± 0.53
7.5%	6.19 ± 0.23	8.57 ± 0.32
10%	9.84 ± 0.06	11.18 ± 0.28
15%	13.3 ± 0.31	14.38 ± 0.13

Also for the other concentrations we observe that the % of flame retardant pick-up after plasma exposition is higher than Nylon samples that are not subjected to He/O_2 gases, i.e. plasma activation leads to a higher absorption of thiourea on the fabric due to the increase content of functional polar groups. Thanks to LOI equipment we will study the flame retardancy properties for all these concentrations and we will evaluate when we can reach the best performances.

5.2.5 LOI Results

In this paragraph we will focus on the LOI test, as explained in § 4.3. In Tab. 5.6 we present LOI values for pure Nylon and for Nylon treated with plasma gases; no thiourea is present on these samples. This test can give information mainly about the initial step of the fire, that is the ignition; a higher LOI value indicates that the specimen does not lead easily to a fire spread.

Tab. 5.6: *LOI values [%], standard deviations* ± 0.2

Name of the sample	LOI [%]
Control sample	35.6
Nylon 66 after plasma	35.3

From these values we conclude that plasma alone does not lead to better fire performances; now we present Tab. 5.7, where we summarise all LOI values for samples treated with thiourea only and for the corresponding samples treated with plasma and then thiourea. Observing the burning of Nylon 66 samples, in general we can say that it degrades by a dripping mode, adding thiourea what changes is drip color (Fig. 5.20), since they become much darker after impregnation in the flame retardant solution.

Tab. 5.7: *LOI values [%], standard deviation* ± 0.2

Thiourea treatment	No plasma	Plasma treatm.
5 %	37.5	38.5
7.5%	40.1	41.7
10%	40.9	42.7
15%	41.5	42.4

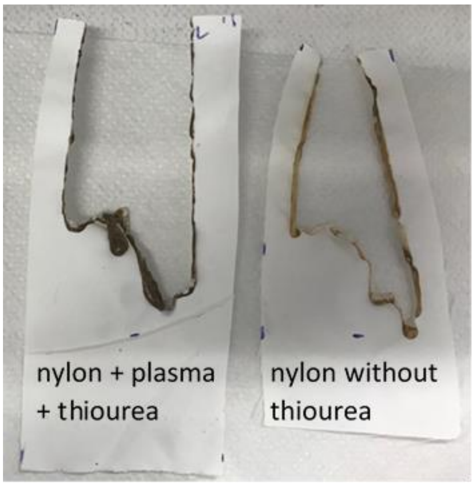

Fig. 5.20: *samples after LOI test*

For the specimen impregnated with 10% thiourea solution, we measured the LOI test for the sample treated with plasma and soaked in the flame retardant solution, but now the difference is that in this case the piece of fabric is not washed as the others with the detergent. LOI value in this case is 42.5 % ± 0.2, almost equal to the washed specimen that is 42.7 ± 0.2. So we can state that it is possible to treat the textile avoiding waste water that derives from the scouring. Indeed plasma is also capable of removing impurities and organic contamination, this effect is called *surface cleaning*. In particular oxygen gas is important for the plasma-clean process [24]. Ablation (or plasma etching) is essential for the elimination of possible weak bond substances present on the surface; the principal advantage of cleaning with plasma is that liquid rinse is not necessary, since it is a dry process.

From Tab. 5.7 we see that LOI values increases when samples are exposed to plasma treatment for all the concentrations, this result agrees with the dry pick-up values reported above; since more flame retardant is attached on samples that are processed in the reactor, LOI increases in the same way. To understand for which concentration we can obtain the best result in this test we show the plot ΔLOI (difference between the LOI of the treated sample and the one of the corresponding fabric not processed in the chamber) versus % of thiourea in Fig. 5.21.
We notice that until 10% increasing the concentration of thiourea, ΔLOI raises, but then at 15% we observe a sudden decrease in ΔLOI, showing the presence of an optimal point for the concentration of this flame retardant, that is 10%. This value leads to the highest fire retardancy performance of Nylon 66, recalling that the parameters used for this study are 2 min for the time treatment, 80 W for the power, and 5 to 1 for the gas ratio.

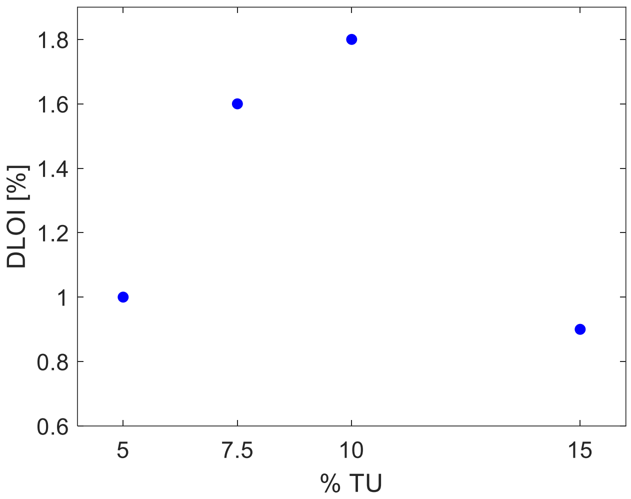

Fig. 5.21: *ΔLOI versus % thiourea in solution*

For this reason we will perform a DOE experiment to understand the best plasma parameters to work with, using a concentration of thiourea equal to 10%. The relative results will be explained in the next chapter.

We have also measured the LOI values using plasma treatment with pure gases: oxygen and helium. In Tab. 5.8 we report the obtained results; we adopt the same parameters for the plasma equipment and a solution of 10% thiourea.

Tab. 5.8: *LOI values [%], standard deviations* ± 0.2

Gas plasma	**LOI [%]**
Helium	41.6
Oxygen	30.7
He/O_2	42.7

We state that for these conditions the best LOI value is obtained with the mixture He/oxygen, and not with single gas. Indeed oxygen generates functional groups that have temporary stability; instead inert gas causes the presence of radicals, but not of functional groups [20], as said in § 5.2.1. To increase surface energy and allow a major adhesion of flame retardant on the fabric it is better to functionalise the material with the mixture.

Chapter 6

Statistical analysis

In this chapter we perform a DOE (*Design of Experiment*) using statistic software, to find the model, if there is, which can describe the relation between the LOI response and two parameters, time and power, considering the vacuum plasma equipment. Secondly, if a model will be found, an optimisation step is required.

6.1 Design of experiment

We want to run a DOE using Design-Expert® software, a statistical program produced by Stat-Ease company. We build a New Design defining the parameters involved in our work. We choose a Response Surface as Study Type, Randomized as Subtype, I-optimal Design Type; in this way we have the possibility to design an experiment where both time and power variables can have discrete values. The Response variable is ΔLOI, indeed we consider the difference of LOI value between the untreated Nylon samples ($LOI = 40.9\% \pm 0.2\%$) and the samples treated with different conditions of gas plasma, both dipped in 10% solution of thiourea. Our purpose is to understand in which conditions we can maximise this variable, obtaining in this way higher fire test performances for our fabric.

We define the minimum, medium and maximum values (3 Levels) of the two discrete factors, as we can see in Fig. 6.1, producing 9 final runs that must be performed (Fig. 6.2). We select 120 and 300 s for time variable because for them we observed higher NPA values, and we choose 30 as the minimum time to perform the study; concerning power values, we opt for 40, 80 and 200 W for the same reason.

After these 9 experiments, we insert the 9 ΔLOI and the program analyses the response.

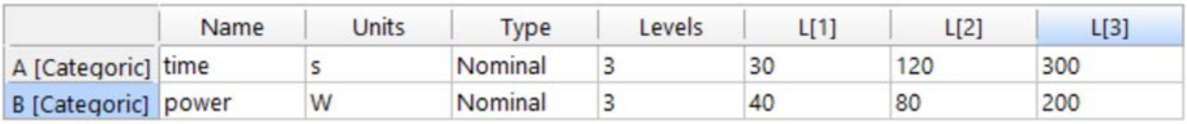

	Name	Units	Type	Levels	L[1]	L[2]	L[3]
A [Categoric]	time	s	Nominal	3	30	120	300
B [Categoric]	power	W	Nominal	3	40	80	200

Fig. 6.1: *3 Levels of the two discrete factors*

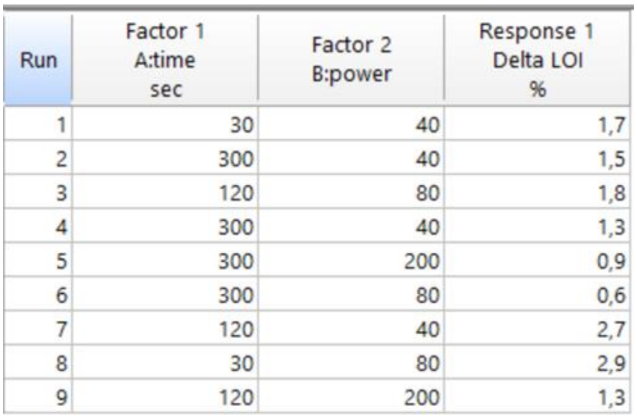

Run	Factor 1 A:time sec	Factor 2 B:power	Response 1 Delta LOI %
1	30	40	1,7
2	300	40	1,5
3	120	80	1,8
4	300	40	1,3
5	300	200	0,9
6	300	80	0,6
7	120	40	2,7
8	30	80	2,9
9	120	200	1,3

Fig. 6.2: *9 Runs performed to study the Response* ΔLOI

6.1.1 Results analysed from the software

From the *Fit Summary* we see that the Linear model is the only one suggested from the software, the Quadratic one is not significant to fit our results;

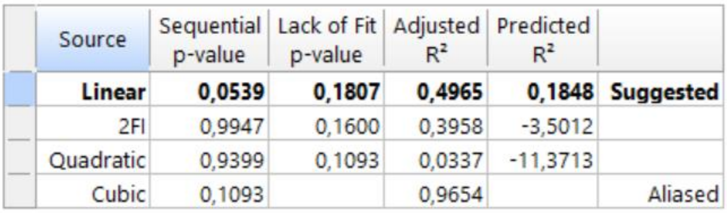

Source	Sequential p-value	Lack of Fit p-value	Adjusted R^2	Predicted R^2	
Linear	**0,0539**	**0,1807**	**0,4965**	**0,1848**	**Suggested**
2FI	0,9947	0,1600	0,3958	-3,5012	
Quadratic	0,9399	0,1093	0,0337	-11,3713	
Cubic	0,1093		0,9654		Aliased

Fig. 6.3: *Fit Summary with the suggested model for this experiment*

The *ANOVA (Analysis of Variance*) reports the following results:

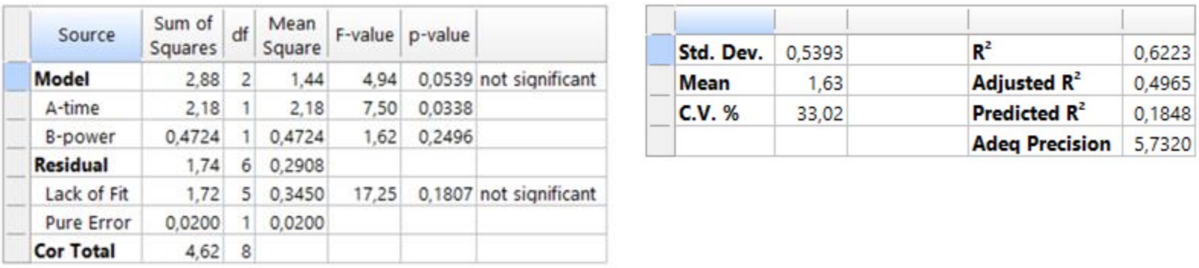

Source	Sum of Squares	df	Mean Square	F-value	p-value	
Model	2,88	2	1,44	4,94	0,0539	not significant
A-time	2,18	1	2,18	7,50	0,0338	
B-power	0,4724	1	0,4724	1,62	0,2496	
Residual	1,74	6	0,2908			
Lack of Fit	1,72	5	0,3450	17,25	0,1807	not significant
Pure Error	0,0200	1	0,0200			
Cor Total	4,62	8				

Std. Dev.	0,5393		**R^2**	0,6223
Mean	1,63		**Adjusted R^2**	0,4965
C.V. %	33,02		**Predicted R^2**	0,1848
			Adeq Precision	5,7320

Fig. 6.4: *ANOVA for Linear Model and R^2 values*

R^2 has a value of 0.6223, so less than 1, it means that the observed response variable is different from the one expected. Moreover, the Predicted R^2 is not close to the Adjusted, they should be within 0.20 of each other; this may indicate a possible problem with the model, we should consider the presence of outliers for example.

P-values less than 0.05 (confidence interval of 95% is chosen by default) indicate model terms that are significant, values higher than 0.1 instead are not significant; in this case A (i.e. time) is significant, not B (i.e. power). Significant model terms probably have a real effect on the response.

We identify the relative impact of time factor higher than power factor.

The final equation in terms of actual factors, that can be used to make prediction about the response for given levels of each factor, is the following:

$$\Delta LOI = 2.757 - 0.004 * time - 0.004 * power \qquad (Eq. 6.1)$$

Now we focus on the *Diagnostic Report* and its graphs; we show in Fig. 6.5 two plots, the first has on y-axis the predicted values (generated using the prediction equation), on x-axis instead the actual ones (measured for that particular run); on the line predicted values are equal to the actual ones, so for the points that lie on the line we can say that the model is well predicting our experimental points. Otherwise this represents how far points are from this line, and so the degree of accuracy of the model.

Regarding the DFFITS index as function of Run number, it measures the influence the ith observation has on the predicted value; it takes into account the Leverage: this number can vary from 0 to 1, if it is 1 the predicted value in that case will exactly equal the observed value of the experiment, and the residual will be 0.

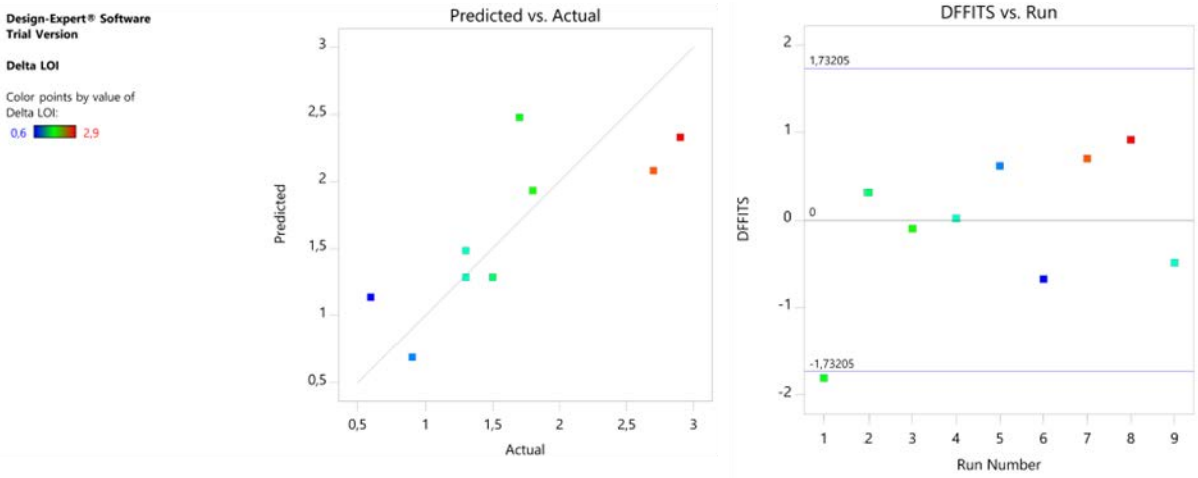

Fig. 6.5: *Diagnostics graphs*

We notice that the linear model does not fit the actual values, as expected from the R^2 value. Moreover, we notice an outlier that exceeds limits [-1.73205, 1.73205], that is the first run. So, what we can do is to perform another statistical analysis ignoring the first experimental value, to understand if the software finds a better regression.

6.1.2 Statistical analysis after ignoring the first Run

From the *Fit Summary* (Fig. 6.6) the suggested model is either Linear or Quadratic; we should focus on the model that maximises the Adjusted R^2, so the Quadratic one. Now AB, A^2, B^2 terms will be included as well.

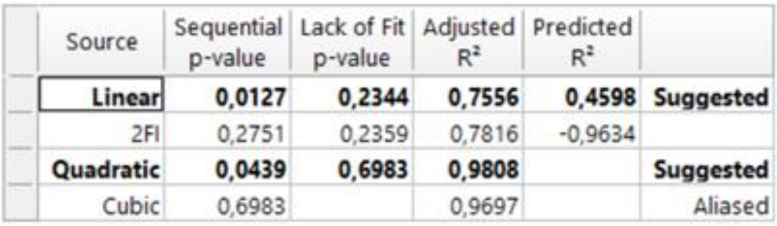

Source	Sequential p-value	Lack of Fit p-value	Adjusted R^2	Predicted R^2	
Linear	**0,0127**	**0,2344**	**0,7556**	**0,4598**	**Suggested**
2FI	0,2751	0,2359	0,7816	-0,9634	
Quadratic	**0,0439**	**0,6983**	**0,9808**		**Suggested**
Cubic	0,6983		0,9697		Aliased

Fig. 6.6*: Fit Summary with the suggested model for this experiment*

The *ANOVA (Analysis of Variance*) displays the following results, collected in Fig. 6.7:

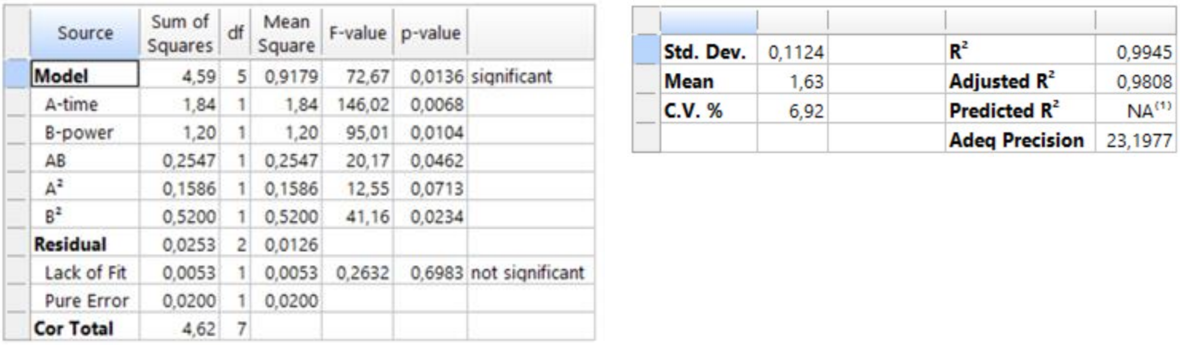

Source	Sum of Squares	df	Mean Square	F-value	p-value	
Model	4,59	5	0,9179	72,67	0,0136	significant
A-time	1,84	1	1,84	146,02	0,0068	
B-power	1,20	1	1,20	95,01	0,0104	
AB	0,2547	1	0,2547	20,17	0,0462	
A^2	0,1586	1	0,1586	12,55	0,0713	
B^2	0,5200	1	0,5200	41,16	0,0234	
Residual	0,0253	2	0,0126			
Lack of Fit	0,0053	1	0,0053	0,2632	0,6983	not significant
Pure Error	0,0200	1	0,0200			
Cor Total	4,62	7				

Std. Dev.	0,1124	**R^2**	0,9945
Mean	1,63	**Adjusted R^2**	0,9808
C.V. %	6,92	**Predicted R^2**	NA⁽¹⁾
		Adeq Precision	23,1977

Fig. 6.7*: ANOVA for Quadratic Model and R^2 values*

All terms, checking the p-values, are significant, only A^2 is a border line term with a p-value of 0.071, but it is less than 0.1, so still acceptable. Here we notice that R^2 is rather close to 1, moreover the Predicted R^2 is not defined, indeed in this case the Leverage is 1.

The final equation in terms of actual factors is indicated in Eq. 6.2:

$$\Delta LOI = 6.036 - 0.019 * t - 0.044 * P + 3.2 * 10^{-5} * t * P + 2.4 * 10^{-5} * t^2 + 12.9 * 10^{-5} * P^2 \qquad (Eq. 6.2)$$

In Fig. 6.8 we show the plot of predicted values of the response versus the actual ones. In this situation we see that the model can fit very well the experimental data since almost all the points are on the line.

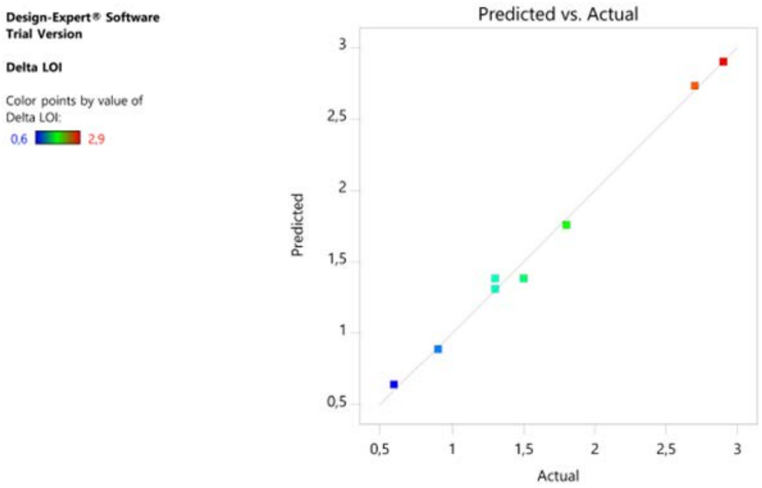

Fig. 6.8: *Diagnostics graph*

In *Model Graphs* we can observe the 2D Surface Response and the 3D one (Fig. 6.9 and 6.10); from *Contour* we select the 2D surface, where we study the time-power dependence and the behaviour of the process. Black bends are parametric with ΔLOI values: for example at a fixed value of power, increasing the treatment time, the response parameter decreases; for a fixed value of time, increasing the power, the response variable decreases as well. To have the same LOI value, when increasing the time it is necessary to decrease the power, and vice versa.

From a physical point of view this means that the Nylon 66 fabric has to be treated at low time and power, indeed higher values of ΔLOI are observed in the red region. The reason could be that, for a prolonged treatment period, etching effects due to superficial interactions can occur, and these cause an increasing of the fabric temperature, destroying the formed functional groups.

Also increasing the power of the plasma more radicals are present, their high concentration can lead to reactions, crosslinking that can produce an opposite effect to the functionalisation [25].

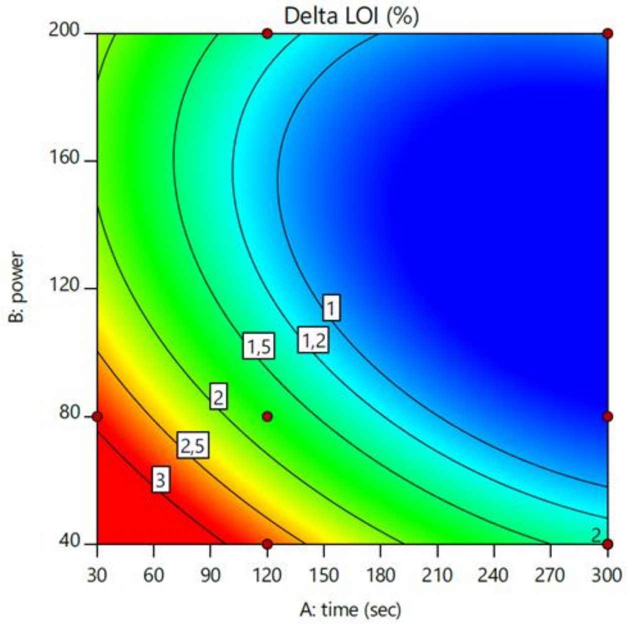

Fig. 6.9: *Contour representation of the process behaviour*

The 3D surface (Fig. 6.10) that displays the relation between these 3 factors is not flat, its curving is due to the relation between time and power, the model indeed does not consider these two factors independent, also their product is involved in the final equation.

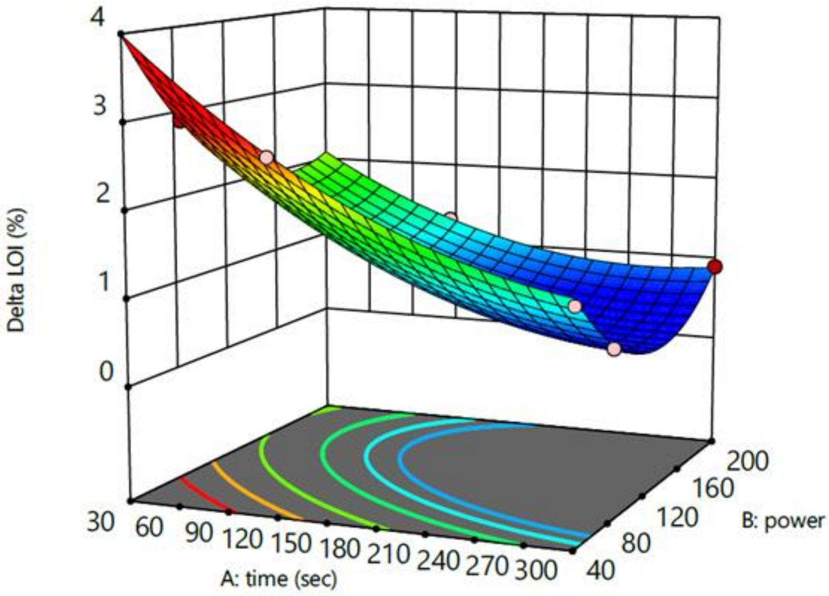

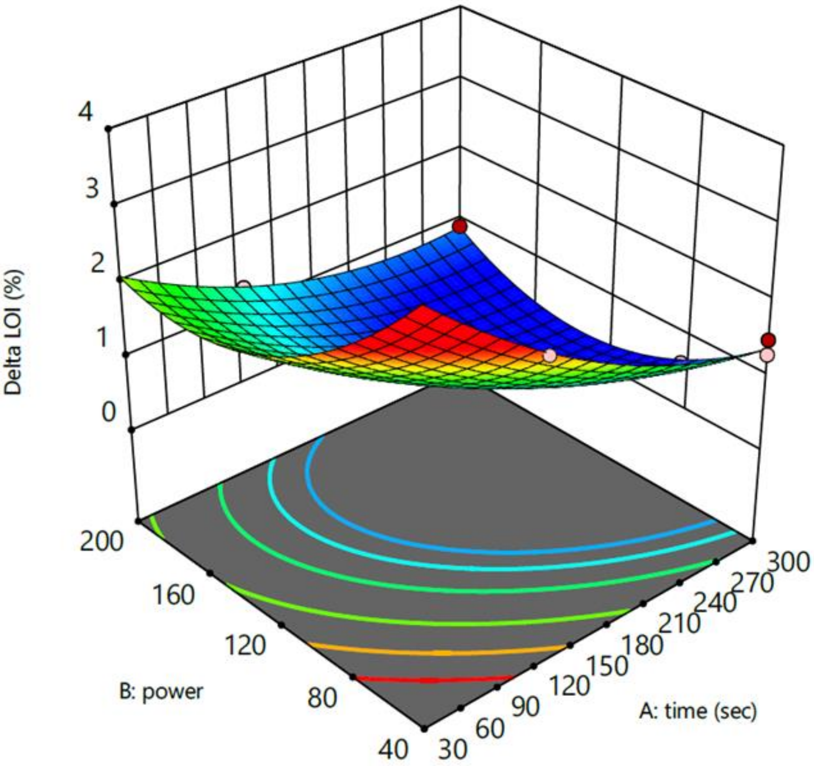

Fig. 6.10: *3D representation of the process behaviour*

6.1.3 Optimisation

In the *Optimization* box we select *Numerical*, in *Criteria* window we maximise the response variable ΔLOI, since this is our goal. To obtain a ΔLOI of about 2.9% we have to perform a last experiment: the software tells us to use a power of **50 W,** with a time of **80 s** (Fig. 6.11). If this happens, it means that the model is predicting well the behaviour of the response parameter.

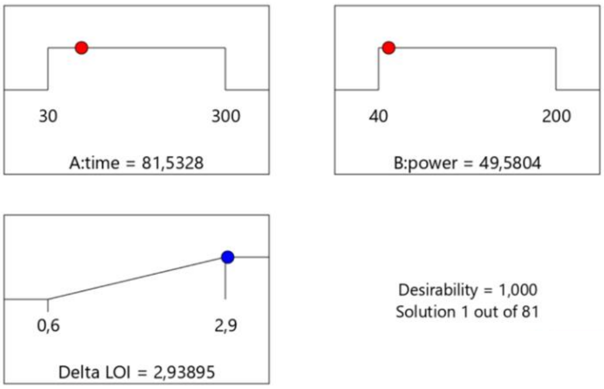

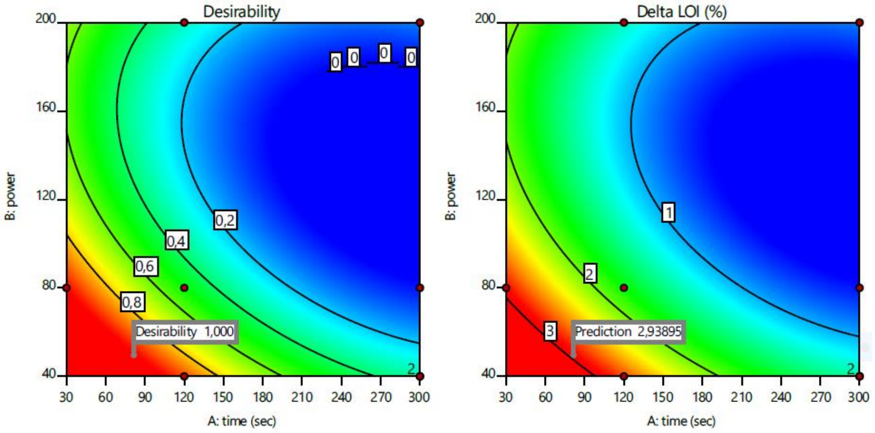

Fig. 6.11: *Optimisation graphical representation*

After performing this last experiment, we state that the obtained value for LOI is 44 ± 0.2, with a ΔLOI of 3.1; considering the standard deviation related to LOI equipment (± 0.2) and the rounding of the power and time parameters, we conclude that the model can well predict LOI values.

Measuring the amount of thiourea present on the samples, these specimens treated with plasma have 11.92 % ± 0.23 of dry pick-up, instead, as mentioned in § 5.2.4, specimens that are not treated with He/O_2 have a LOI of 9.84% ± 0.06.

6.1.4 FTIR Spectra after soaking in thiourea solution

The optimized sample has also been characterized by FTIR. In Fig. 6.12 we show FTIR spectrum of Nylon fabric soaked in 10% solution of thiourea compared to the spectrum of pure Nylon 66; the goal is to show the new peaks that appear after dipping the textile into flame retardant solution.

We observe a new peak at 1083 cm^{-1}, it represents the C=S stretching that is the bond present in thiourea molecule. A more accentuated peak is the one at around 727 cm^{-1}, that probably indicates the presence of C-N single bond, present in thiourea structure [26]. Also we notice different intensities of the peaks that appear in the region 1475-1370 cm^{-1}, area that belongs to C-H bending.

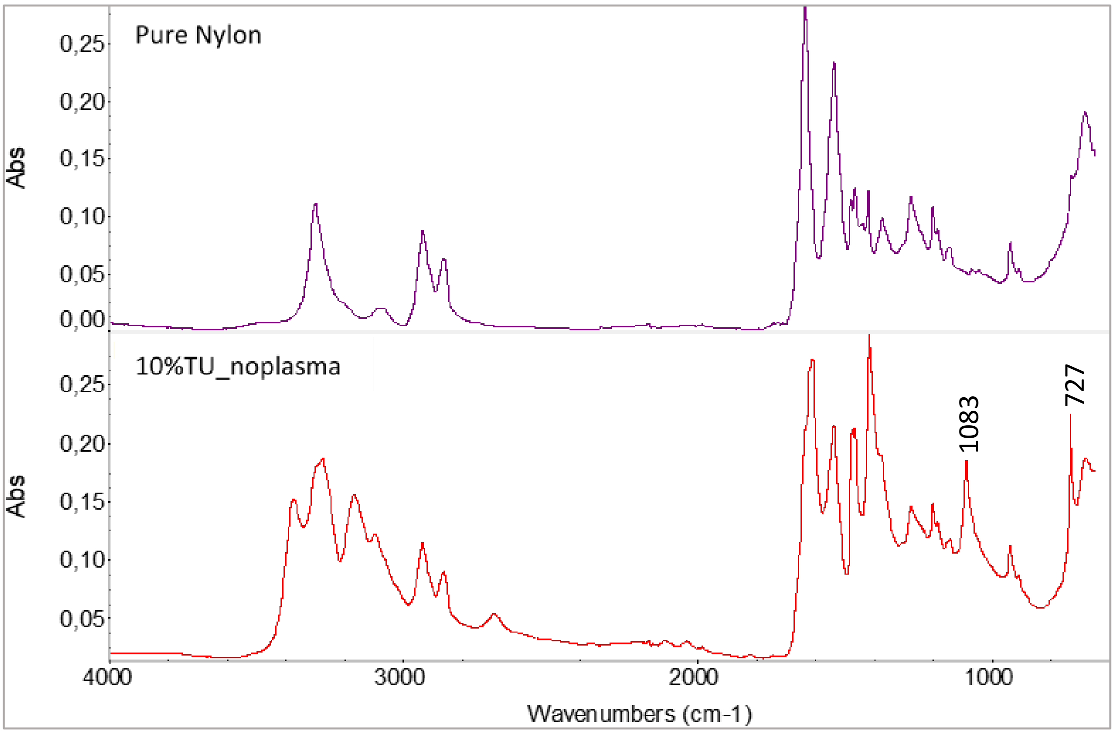

Fig. 6.12: *Comparison between pure Nylon and dipped Nylon spectra*

As follows we report two FTIR spectra, where we compare the spectrum of Nylon dipped in 15% solution of thiourea without plasma treatment, and the one soaked in the solution after plasma treatment. Plasma conditions are 80 s and 50 W, as suggested by the Optimisation. Here we choose a concentration of 15% because it is more evident from these FTIR results the distinction between the two spectra, compared to 10% analyses.

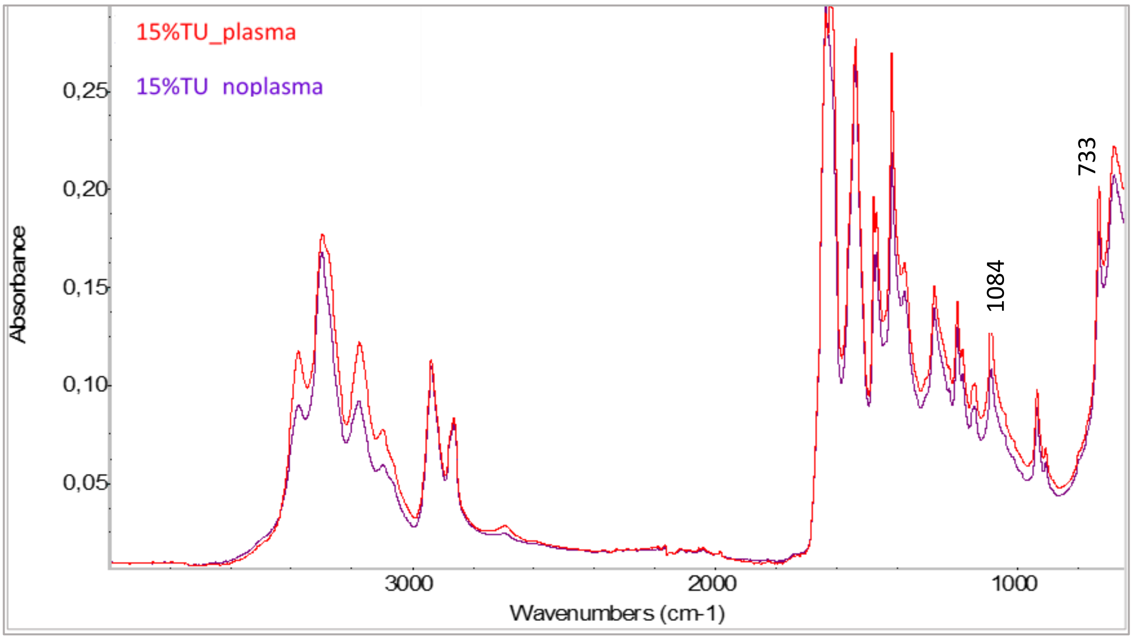

Fig. 6.13: *Comparison between the sample treated with plasma and TU and the one with just TU*

Since N-H bending has a peak present on Nylon 66 spectrum but not in the thiourea one, we consider it as a reference peak for the calculation of NPA value for samples soaked in thiourea solution. In Tab. 6.1 we compare these values for the two samples analysed in Fig. 6.13.

Tab. 6.1: *NPA values for samples soaked in 15% thiourea solution*

Absorbance [cm^{-1}]	No plasma	Plasma treatm.
1084 (C=S)	0.27	0.32
733 (C-N)	0.23	0.24

We conclude that, according to the results presented in the previous chapter, more flame retardant is attached on Nylon surface after plasma treatment; this can be seen from dry add on results, LOI values and in addition, from FT-IR spectra reported above. NPA values calculated in Tab. 6.1 show that C=S bond has a higher absorption after plasma treatment.

DOE experiment has allowed us to find the best conditions to process this textile in order to increase flame retardancy performances, and this can be seen from the final LOI value that is obtained with 80 s and 50 W. Then we have proved that also in this case the increase of LOI after plasma process is due to a higher amount of thiourea attached on the fabric.

6.1.5 SEM images for the optimised treatment

Fig. 6.14 shows the SEM images of Nylon treated for 80 s and at 50 W. We see that at low power and for a short treatment time slits and grooves are not observed on the fibres, we do not observe pronounced modifications on the morphological structure, but rather a regular surface.

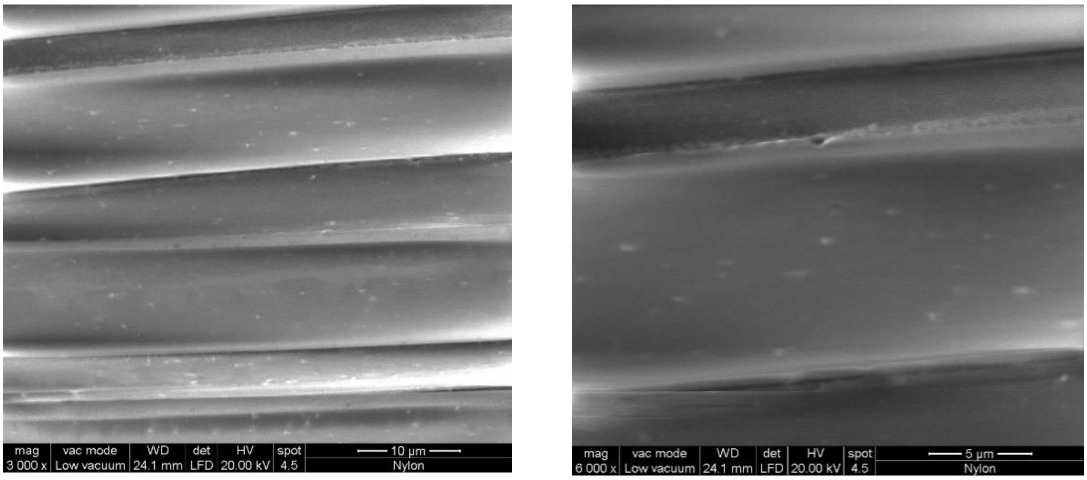

Fig. 6.14: *SEM images of sample treated for 80 s at 50 W*

Conclusions

The main objective of this work has been the enhancement of the flame retardancy of Nylon 66 textile by improving the effectiveness of the flame retardants treatment, i.e. the amount of flame retardant uptake, by using plasma functionalization, both atmospheric and vacuum one.

Regarding the atmospheric instrument we can assess that this type of plasma, for both gases tested (Ar and O_2), is not working well on this fabric, since the treatment is not homogenous and leads to no variation in the surface composition. Also from the SEM images we can conclude that not pronounced grooves are detected, while the plasma should lead to a rougher surface, that in this case is not observed. For this reason we have decided to proceed analysing deeply the vacuum plasma instrument, which though has higher costs and this is its main limitation.

From preliminary test, based on the capillarity test and the FT-IR spectra results, we have decided to treat the fabric with the microwave vacuum plasma for 2 min, at 80 W and with a gas ratio for the mixture He/O_2 equal to 5:1. These results have also proved that vacuum plasma caused a more homogeneous treatment, with respect to the atmospheric instrument.

Then it has been shown that, whatever the thiourea concentration used in the finishing solution, plasma treated textile exhibited a higher thiourea uptake and, therefore, a higher limiting oxygen index. The greatest difference between functionalized and un-functionalized samples has been obtained for 10% thiourea solution, for which the dry add-on increased from 9.84% for the control sample (no plasma,) to 11.18% for the sample treated by plasma. The resulting LOI is 40.9 ± 0.2 for the control specimen and 42.7 ± 0.2 for the treated one.

Finally, DOE investigation was performed varying time and power variables, where the response parameter is ΔLOI, i.e. the difference in LOI between control and plasma-treated sample. A quadratic model fit the data in a good way, with the R^2 equal to 0.9945. Using the model, from the contour representation and the 3D graph, it can be seen that treating the fabric at low times and powers improved the performance, since in this way we can avoid etching effects or the cross-linking of radicals. The optimisation suggested by the software was experimentally verified and treating nylon textile for 80 s and 50 W, with a 5:1 He/O_2 mixture a LOI of 44 ± 0.2 was obtained.

In conclusion, we affirm that the goal is reached, fire retardancy performances after plasma treatment can increase, thanks to a major uptake of thiourea on the surface.

Future studies should be done to find an atmospheric machine that can generate an efficient treatment on the fabric, so that more flame retardant can be add on Nylon surface, decreasing the costs related to this procedure. A further improvement should be obtained avoiding completely the wet finishing process, thus avoiding the generation of wastewater. A new mode of applying the flame retardant on textiles is its vaporisation simultaneously with the plasma process. In this way it may create free radicals on the surface, which may form covalent bonds with the flame retardant introduced in the same equipment. In Huddersfield (UK) it is present a patented apparatus that can treat at atmospheric pressure the material and dispense the finishing right after the plasma activation; future work is needed to understand if it can actually work.

References

[1] A. F. Holdsworth, “Novel Metal Complex Fire Retardants for Engineering Polymers,” Ph.D. thesis, University of Bolton, 2015.

[2] C. A. Wilkie, and A. B. Morgan, “Fire Retardancy of polymeric Materials: 2nd Edition,” ch. 2, pp. 15-42, CRC Press, Boca Raton, 2010.

[3] L. H. Peebles, JR., and M. W. Huffman, “Thermal Degradation of Nylon 66,” *J. Polym. Sci.*, vol. 9, no. 7, pp. 1807–1822, 1971.

[4] P. N. Thanki, and R. P. Singh, “Photo-oxidative degradation of nylon 66 under accelerated weathering,” *Polymer*, vol. 39, no. 25, pp. 6363–6367, 1998.

[5] D. Zavattini, “I filati di nylon 6,6: lavorazioni e caratteristiche principali, applicazioni e valutazione ambientale del ciclo produttivo,” tesi di laurea in Ingegneria dei Materiali, Università degli Studi di Padova, 2011.

[6] H. Conrads, and M. Schmidt, “Plasma generation and plasma sources,” *Plasma Sources Sci. Technol.*, vol. 9, no. 4, pp. 441–454, 2000.

[7] A. Sparavigna, “Plasma treatment advantages for textiles,” arXiv:0801.3727, 2008.

[8] C. W. Kan, and W. S. Man, “Surface characterisation of atmospheric pressure plasma treated cotton fabric-Effect of operation parameters,” *Polymers*, vol. 10, no. 3, pp. 250-264, 2018.

[9] K. B. Gilleo, “Nylon Flammability-Effects of Thiourea, Ammonium Sulfamate, and Halogen Compounds,” *Ind. Eng. Chem. Prod. Res. Develop.*, vol. 13, pp. 139-143, 1974.

[10] E. D. Weil, and S. V. Levchik, “Flame Retardants for Plastics and Textiles,” Hanser Publications, Ohio, 2009.

[11] A. R. Horrocks, “Flame retardant challenges for textiles and fibres: New chemistry versus innovatory solutions,” *Polym. Degrad. Stab.*, vol. 96, no. 3, pp. 377–392, 2011.

[12] “BS EN ISO 4589 - 2 : 2017 BSI Standards Publication Plastics — Determination of

burning behaviour by oxygen index," 2017.

[13] K. H. Kale, and A. N. Desaia, "Atmospheric pressure plasma treatment of textiles using non-polymerising gases," *Indian J. Fibre Text. Res.*, vol. 36, no. 3, pp. 289–299, 2011.

[14] S. E. More, P. S. Das, A. Bansode *et. al.*, "Diagnostics of microwave assisted electron cyclotron resonance plasma source for surface modification of nylon 6," *Rev. Sci. Instrum.*, vol. 89, no. 1, 2018.

[15] E. N. Hristea, M. T. Caproiu, G. Pencu, and M. Hillebrand, "and HOO – Radicals and Anions," *Int. J. Mol. Sci.*, vol. 7, pp. 130–143, 2006.

[16] B. Ozcelik, J. H. Lee, and D. B. Min, "Effects of Light , Oxygen , and pH on the Effects of Light , Oxygen , and pH on the Absorbance of 2 , 2-Diphenyl-1-picrylhydrazyl," *J. of Food Chem. and Techn.*, vol. 68, no. July 2006, pp. 487–490, 2014.

[17] A. G. J. Ghadam, and H. Karimi, "Synthesis and Characterization of Polyamide-66/Calcium Carbonate Composites, " *J. of Chem. and Petr. Engin.*, vol. 49, no. 1, pp. 63-78, 2015.

[18] A. Haji, A. Mousavi Shoushtari, and M. Mirafshar, "Natural dyeing and antibacterial activity of atmospheric-plasma-treated nylon 6 fabric," *Color. Technol.*, vol. 130, no. 1, pp. 37–42, 2014.

[19] W. Zhang, L. Johnson, S. R. P. Silva, and M. K. Lei, "The effect of plasma modification on the sheet resistance of nylon fabrics coated with carbon nanotubes, " *Appl. Surf. Sci.*, vol. 258, pp. 8209-8213, 2012.

[20] C. M. Chan, T. M. Ko, and H. Hiraoka, "Polymer surface modification by plasmas and photons," *Surf. Sci. Rep.*, vol. 24, no. 1–2, pp. 1–54, 1996.

[21] G. Rosace, and R. Canton, "Influence of Low-Temperature Plasma Conditions on Wicking Properties of PA/PU Knitted Fabric, " *J. Appl. Sci.*, vol. 107, pp. 3702-3706, 2007.

[22] W. J. Sichina, "Characterization of Polymers Using TGA," *Therm. Anal.*, pp. 1–4, 2011.

[23] K. R. Millington, G. Maurdev, and M. J. Jones, "Mechanism of photoprotection of wool with formaldehyde and thiol derivatives," *Color. Technol.*, vol. 125, no. 2, pp. 117–122, 2009.

[24] M. Strobel, C.S. Lyons, and K. L. Mittal, “Plasma Surface Modifications of Polymers: Relevance to Adhesion,” CRC Press, New York, 2018.

[25] U. Cvelbar, “Interaction of non-equilibrium oxygen plasma with sintered graphite,” *Appl. Surf. Sci.*, vol. 269, pp. 33–36, 2013.

[26] C. Hampton, and D. Demoin, “Vibrational Spectroscopy Tutorial: Sulfur and Phosphorous” https://faculty.missouri.edu/~glaserr/8160f10/A03_Silver.pdf, accessed on 15th September 2018.

Acknowledgments

First of all, I would like to thank Prof. Lorenzetti for her support and her precious advices within these months. Also, I thank her for the opportunity to work abroad at University of Bolton.

Here I had the possibility to meet Prof. Kandola and Prof. Horrocks, that have explained me the principles of plasma equipment and of flame retardants. Moreover, another important person was my patient and sweet tutor Maram, that has always reassured me in the difficult moments. Then, I would like to thank all the PhD students and the technician John of the fire office, with which I have spent happy moments.

Thank you also to my flat mates Zhishi and Maira, I will miss you.

Proseguo con il ringraziare le persone che ho incontrato nel laboratorio di polimeri all'Università di Padova; ringrazio Elena per la sua disponibilità e il tempo dedicatomi, Romeo per avermi insegnato ad usare i vari strumenti, Carlo e Martina per la loro gentilezza nel risolvere i problemi incontrati durante questo percorso. Inoltre ringrazio Lorenza che con le sue schiume mi ha fatto compagnia nelle giornate di laboratorio, tutti i tesisti e dottorandi dell'ufficio per i momenti spensierati e i mega pranzi trascorsi insieme.

Dei ringraziamenti speciali vanno ai miei genitori e mio fratello Michele, senza il loro aiuto economico e soprattutto emotivo non avrei mai raggiunto questo importante traguardo.

Questo percorso è stato più spensierato grazie ai compagni di corso che in questi anni sono diventati anche degli amici. In particolare grazie Deborah, insieme a te tutti i pomeriggi di studio, i lavori di gruppo sono stati più divertenti, e grazie per le ore di chiacchierata su Skype quando avevo bisogno di una parola di conforto.

Grazie ai miei pazzi coinquilini Martina, Chiara e Leonardo e alle nostre 'serate pizza'.

Vorrei poi ringraziare le mie amiche Vanessa, Sara, Valentina, Gioia, Bonnie per aver tollerato i miei momenti di assenza ed esserci da sempre.

Per ultimo, ma più importante, ringrazio Filippo, solo tu e mamma Daniela potevate sopportare tutte le mie ansie e spingermi sempre ad andare avanti con entusiasmo.